

1  
2  
3 1 **CARBON-ISOTOPE ANOMALIES AND DEMISE OF CARBONATE PLATFORMS IN THE**  
4  
5 2 **SINEMURIAN (EARLY JURASSIC) OF THE TETHYAN REGION: EVIDENCE FROM THE**  
6  
7 3 **SOUTHERN ALPS (NORTHERN ITALY)**  
8  
9  
10 4

11 5 **DANIELE MASETTI\*\***, **BILLY FIGUS\***, **HUGH C. JENKYNs°**, **FILIPPO BARATTOLO\*\*** and **RENATO**  
12  
13  
14 6 **POSENATO\***  
15  
16  
17 7

18 \*Dipartimento di Fisica e Scienze della Terra, Università degli Studi di Ferrara, Polo  
19 scientifico-tecnologico, Via Giuseppe Saragat 1, 44122 Ferrara, Italy  
20  
21  
22

23 10 °Department of Earth Sciences, University of Oxford, South Parks Road, Oxford OX1 3AN, UK  
24

25 11 \*\* Dipartimento di Scienze della Terra, Università degli Studi di Napoli, Largo San Marcellino 10, 80138  
26  
27 12 Napoli, Italy  
28  
29  
30  
31  
32  
33

34 15 Keywords: Carbon-isotope anomalies; carbonate platform demise; Tethyan continental margins;  
35  
36 16 Jurassic, Southern Alps; Northern Italy.  
37  
38  
39  
40  
41  
42

43 18 **INDEX**

44 19 **ABSTRACT**

45 20 **1.0 INTRODUCTION: THE DEMISE OF CARBONATE PLATFORMS DURING THE SINEMURIAN IN THE TETHYAN AREA.**

46  
47 21 **2.0 GEOLOGICAL SETTING: THE SOUTHERN ALPS**

48  
49 22 **2.1 The Trento Platform**

50  
51 23 **2.2. The Belluno Basin**

52  
53 24 **2.3. The Friuli Platform**

54  
55  
56 25 **3.0 CHEMOSTRATIGRAPHIC TRANSECT ACROSS THE EASTERN SOUTHERN ALPS**

57  
58 26 **3.1 Chemostratigraphic sampling**  
59  
60

1  
2  
3 27 **3.2 The Monte Verzegnis section**

4  
5 28 **3.3 The Monte Cumieli section**

6  
7 29 **3.4 The Foza section**

8  
9 30 **3.5 The Chizzola section**

10  
11 31 **3.6 Correlation of  $\delta^{13}\text{C}$  curves across the Eastern Southern Alps and their comparison with**  
12  
13 **coeval anomalies**

14  
15 32  
16 33 **4.0 POSSIBLE CAUSES OF THE “ARNIOCERAS TIME” NEGATIVE  $\delta^{13}\text{C}$  EXCURSION**

17  
18 34 **5.0 IMPACT OF THE “ARNIOCERAS TIME” NEGATIVE  $\delta^{13}\text{C}$  EXCURSION ON CARBONATE SEDIMENTATION**

19  
20 35 **6.0 SUMMARY AND CONCLUSIONS**

21  
22 36 **7.0 REFERENCES**

23  
24  
25 37

26  
27 38

28  
29 39 **Abstract**

30  
31  
32 40 Despite its global impact on ecosystems, the T/J boundary event had only a modest effect on the  
33  
34 41 carbonate depositional systems of the Southern Alps, whereas a fundamental reorganization of  
35  
36 42 the same palaeogeographic area took place during the Sinemurian Stage. This paper  
37  
38 43 investigates whether or not the well-documented demise of Sinemurian carbonate platforms in  
39  
40 44 the Tethyan region was a response to a global event by examination of carbon-isotope  
41  
42 45 anomalies in successions of different facies that record this interval of time. A chemostratigraphic  
43  
44 46 transect from the Garda Lake up to the eastern Italian border is illustrated by four stratigraphic  
45  
46 47 sections; high-resolution (20 cm over key intervals) chemostratigraphic sampling allowed  
47  
48 48 detection of a major negative  $\delta^{13}\text{C}$  anomaly of  $\sim 1.5\text{‰}$ , preceded by a positive excursion, both in  
49  
50 49 shallow- and deep-water successions, over the stratigraphical range of the ammonite genus  
51  
52 50 *Arnioceras*. A comparison with sections from the UK suggests that the positive excursion  
53  
54 51 belongs to the *turneri* Zone and the succeeding negative excursion falls within the *obtusum*  
55  
56 52 Zone. In the deep-water Belluno Basin, the negative anomaly occurs in a biogenic chert-rich unit  
57  
58  
59  
60

1  
2  
3 53 recording the onset of mesotrophic conditions in the basin. In the platform-carbonate  
4  
5 54 successions, this major negative carbon-isotope excursion is developed within a calcarenitic unit  
6  
7 55 corresponding to the lowest occurrence of the foraminifer *Paleomayncina termieri*. This evidence  
8  
9  
10 56 for deepening and transgression across the carbonate platform suggests pre-conditioning for  
11  
12 57 drowning. Hence, rather than tectonic subsidence alone, environmental factors may have aided the  
13  
14 58 demise of Tethyan carbonate platforms during the Early Jurassic Sinemurian Stage.  
15  
16  
17 59

## 60 **1. INTRODUCTION: THE DEMISE OF CARBONATE PLATFORMS IN THE SINEMURIAN OF THE TETHYAN AREA.**

61 Global episodes of environmental change represent major turning points in the history of the  
62 Earth. Among these, the Triassic/Jurassic boundary (T/J) is characterized not only by a major  
63 extinction but also by disturbances in the carbon-isotope reservoir of the oceans and atmosphere.  
64 Despite its global impact, the T/J event had only a modest effect on the palaeogeographic configuration  
65 of the Southern Alps as exposed in northern Italy. The palaeogeography of the Southern Alps at the  
66 beginning of the Jurassic was characterized by the widespread development of shallow-water  
67 carbonate platforms (Corna, Monte Zugna Formation), representing the continuation of late Triassic  
68 peritidal sedimentation, and stretching from Lombardy to Slovenia, only interrupted by the deep  
69 Belluno Basin (Gaetani, 1975; Winterer and Bosellini 1981; Masetti *et al.*, 2012). Similar shallow-water  
70 environments also existed elsewhere, for example in the Umbria–Marche Apennines of central Italy  
71 (Calcare Massiccio Formation), and in the Southern Limestone Apennines (Calcare a Paleodasycladus  
72 Formation: D'Argenio *et al.*, 1973).

73 Although the T/J event had negligible effect on the Jurassic depositional systems of the Southern Alps  
74 and Apennines, a fundamental reorganization of the carbonate systems took place during Sinemurian  
75 time (Masetti *et al.*, 2012). In Lombardy, the Corna Platform was locally capped by open-marine  
76 crinoidal calcarenites (encrinites) of Sinemurian age (Schirrolli, 1997; Meister *et al.* 2009); across much  
77 of the Trento Platform, the Hettangian–Sinemurian peritidal succession of the Calcari Grigi Group

1  
2  
3 78 (Monte Zugna Fm.) is unconformably overlain by a Sinemurian–Pliensbachian condensed succession  
4  
5 79 (Fanes Piccola Encrinite, Masetti and Bottoni 1975; Masetti *et al.* 2012); in the Northern Apennines,  
6  
7 80 Marino and Santantonio (2010) describe the Early Sinemurian replacement of the peritidal Calcare  
8  
9 81 Massiccio platform by means of deep-water deposits of the Corniola Fm. In the structural highs of the  
10  
11 82 same area this event is recorded later, at the base of the *semicostatum* Zone, by the superposition of a  
12  
13 83 “drowning succession” (“Calcare Massiccio B”) over the underlying, peritidal, “Calcare Massiccio A”. In  
14  
15 84 the Ligurian Alps, the Early Sinemurian carbonate platform ceased sediment production and was  
16  
17 85 covered by deep-water deposits (Decarlis and Lualdi, 2010); in Eastern Sicily, the progradational trend  
18  
19 86 of the peritidal Inici Fm. ceased at the Early/Late Sinemurian boundary, just before the drowning of the  
20  
21 87 carbonate platform that occurred in the Late Sinemurian, when the deep-water Modica Fm. started to  
22  
23 88 accumulate (Ronchi *et al.*, 2000). Ammonites found close to the top of the Inici Formation in western  
24  
25 89 Sicily also suggest that the carbonate platform, locally at least, ceased deposition at some point in the  
26  
27 90 *bucklandi* or *semicostatum* Zone of the Early Sinemurian or soon thereafter (Wendt, 1969; Jenkyns and  
28  
29 91 Torrens, 1971). In the Betic Cordillera (Spain) Ruiz-Ortiz *et al.* (2004) described the Early Jurassic  
30  
31 92 stratigraphic evolution of the rifted Iberian margin indicating that widespread peritidal carbonates  
32  
33 93 evolved with faulting to a more open and deep marine setting. These authors refer the first dissection of  
34  
35 94 the platform by extensional faults to the Early Pliensbachian, on the base of a benthic foraminiferal  
36  
37 95 association. However, prior interpretations have dated the faulting as intra-Sinemurian (Ruiz-Ortiz *et*  
38  
39 96 *al.*, 2004), so the evolution may be similar to the Italian examples. In the High Atlas (Morocco)  
40  
41 97 Merino-Tomé *et al.* (2012) described in detail the break-up of the peritidal Early Jurassic carbonate  
42  
43 98 platform of Djebel Bou Dahar into smaller deeper water blocks as a result of tectonic processes at the  
44  
45 99 boundary between the Early and Late Sinemurian. The same authors highlight a sudden  
46  
47 100 contemporaneous decrease in carbonate production leading to the generalized developing of hiatuses  
48  
49 101 and the subsequent onset, in the Late Sinemurian–Pliensbachian, of sub-photic siliceous sponge  
50  
51 102 microbial facies. Despite the huge increase in area affected by drowning of carbonate platforms in the  
52  
53 103 Apennines and Southern Alps, the consensus to date is to view this event as regional and essentially  
54  
55  
56  
57  
58  
59  
60

1  
2  
3 104 due to increasing subsidence rate of fault-bounded blocks during extension of the Jurassic continental  
4  
5 105 margin (Bernoulli and Jenkyns, 1974).  
6

7 106 Bearing in mind the widespread demise/drowning of carbonate platforms in the Tethyan area during a  
8  
9 107 poorly dated interval or intervals in the Sinemurian, and that the Southern Alps contain outcrops of a  
10  
11 108 former passive Mesozoic continental affected by such phenomena, the main aims of this paper are:  
12  
13 109 1) to investigate whether or not the demise of Sinemurian carbonate platforms was the result, wholly or  
14  
15 110 partially, of a chemostratigraphic/palaeoenvironmental event, by examining carbon-isotope anomalies  
16  
17 111 in successions across the whole area of the eastern Southern Alps;  
18  
19 112 2) to provide high-resolution correlation between shallow-water platform carbonates and deeper water  
20  
21 113 pelagic ammonite-bearing successions across the Eastern-Southern Alps by means of carbon  
22  
23 114 isotopes, in order to locate the exact position/timing of any palaeoenvironmental event.  
24  
25 115 3) to ascertain the nature of carbonate-platform evolution coincident with this palaeoenvironmental  
26  
27 116 event in order to highlight the potential response of the sediment-producing carbonate factory.  
28  
29  
30  
31  
32 117

## 33 34 118 **2. GEOLOGICAL SETTING: THE SOUTHERN ALPS**

35  
36 119 Since the early seventies, the Southern Alps have been interpreted as a passive continental margin  
37  
38 120 that, during Mesozoic time, experienced polyphase extensional tectonics that caused the  
39  
40 121 fragmentation of the Adriatic Plate. The tectonic activity started during the Late Triassic (Norian). After  
41  
42 122 relative quiescence during the Rhaetian (latest Triassic), renewed extension took place during the  
43  
44 123 Early Jurassic. Extension shifted westwards to the Ligurian–Piedmont area where oceanic crust had  
45  
46 124 formed by the Middle Jurassic (Bill *et al.*, 2001). From this time until the Early Cretaceous, the Southern  
47  
48 125 Alps underwent post-rift thermal subsidence (Bertotti *et al.*, 1993; Fantoni and Scotti, 2003).  
49  
50 126 The Mesozoic extension resulted in the creation of N–S half-grabens, bounded by east- and  
51  
52 127 west-dipping master normal faults (Fig.1). In the eastern Southern Alps three  
53  
54 128 paleogeographical-structural units are recognizable. These are, from west to east (Gaetani, 1975;  
55  
56 129 Winterer and Bosellini, 1981): a carbonate platform, which drowned in the Early Jurassic, evolving into  
57  
58  
59  
60

1  
2  
3 130 a pelagic plateau with condensed pelagic sedimentation during the Late Jurassic (Trento Platform) and  
4  
5 131 bordered to the west by the Lombardian Basin that accumulated pelagic clays and carbonates; a basin,  
6  
7 132 with similar pelagic facies, that developed in the very Early Jurassic (Belluno Basin); and a carbonate  
8  
9 133 platform that persisted from the Jurassic till the Cretaceous (Friuli Platform).

## 11 134 **2.1. The Trento Platform**

12  
13  
14 135 On the Trento Platform, the shallow-water sedimentation of the Early Jurassic is recorded in the thick  
15  
16 136 pile of the Calcarei Grigi Group, and the overlying pelagic “condensed” sedimentation recorded by the  
17  
18 137 Rosso Ammonitico Veronese (Bajocian to Tithonian, Fig. 2). The Calcarei Grigi Group is several  
19  
20 138 hundred metres thick; its lower part corresponds to the Monte Zugna Formation, a unit representing the  
21  
22 139 Jurassic continuation of the underlying, Upper Triassic, peritidal succession of the Dolomia Principale.  
23  
24 140 The Loppio Oolitic Limestone and the Rotzo Formation represent, respectively, the middle and upper  
25  
26 141 part of the Calcarei Grigi Group; the most typical and renowned facies are those present in the Rotzo  
27  
28 142 Formation, characterized by abundant plant remains and extensive banks of oyster-like “*Lithiotis*”,  
29  
30 143 deposited in a dominantly subtidal environment (Masetti *et al.*, 1998; Posenato and Masetti 2012;  
31  
32 144 Franceschi *et al.*, 2014). This subtidal environment, interpreted by previous authors as lagoonal, as the  
33  
34 145 so-called “Lithiotis Lagoon” (Bosellini and Broglio Loriga, 1971), passed laterally to the western  
35  
36 146 marginal oolitic complex (Massone Oolite, Figs 2 and 3). The Monte Zugna Formation and the Loppio  
37  
38 147 Oolitic Limestone, lacking faunas of proved chronostratigraphic value, have been referred to a generic  
39  
40 148 Hettangian–Sinemurian p.p. interval, whereas the age of Rotzo Formation is still debated and ascribed  
41  
42 149 to a time interval spanning the late Sinemurian to late Pliensbachian, on the base of foraminifer  
43  
44 150 bio-chronostratigraphy (Fugagnoli, 2004), or to early Pliensbachian to late Pliensbachian, on the base  
45  
46 151 of ammonoid bio-chronostratigraphy (Sarti in Posenato and Masetti, 2012).

51  
52 152 The unconformity surface capping the top of the shallow-water Calcarei Grigi Group corresponds to a  
53  
54 153 temporal hiatus that expands in duration eastward (Masetti *et al.*, 1998; Figs 2 and 3). Based on the  
55  
56 154 hiatus at the top of the Calcarei Grigi Group and the lateral variations displayed by the Pliensbachian  
57  
58 155 units, Masetti *et al.* (2012) proposed a further subdivision of the Trento Platform into a central-western

1  
2  
3 156 area (with the Pliensbachian Rotzo Formation) and in a north-eastern area (without the Rotzo  
4  
5 157 Formation). The approximate spatial distribution of these areas is shown in Figure 2; Figure 3 illustrates  
6  
7 158 the Hettangian–Sinemurian Monte Zugna Formation crossing the entire Trento Platform from west to  
8  
9 159 east with little variation in facies and thickness (Masetti *et al.*, 1998), whereas the classic Calcarei Grigi  
10  
11 160 succession with its well-known “*Lithiotis*” beds (Rotzo Formation) is present only in the central-western  
12  
13 161 sector of the Trento Platform passing westward to plane-bedded facies interpreted as marginal shoals  
14  
15 162 (Massone Oolite; Beccarelli-Bauch, 1988).

16  
17  
18 163 The north-eastern sector of the Trento Platform (Figs 2 and 3) is characterized by a widespread hiatus  
19  
20 164 corresponding to the Pliensbachian units, replaced by a thin veneer of red cross-bedded crinoidal sand  
21  
22 165 bodies corresponding to the Fanes Piccola Encrinite: where this unit is missing, the Rosso Ammonitico  
23  
24 166 rests directly on the Monte Zugna Formation (Masetti *et al.*, 2012).

25  
26  
27 167

28  
29  
30 168

## 31 32 33 169 **2.2. The Belluno Basin.**

34  
35 170 The birth of the Belluno Basin was linked to Early Jurassic rifting that led to a roughly N–S oriented fault  
36  
37 171 system (Masetti and Bianchin, 1987); during Hettangian–Pliensbachian time, this basin was filled by  
38  
39 172 dark cherty, basinal micrites (Soverzene Formation, Figs 2, 3). On the base of data coming from the  
40  
41 173 Verzegnis section, where sediments are free from heavy dolomitization, Masetti *et al.* (2012)  
42  
43 174 suggested that the birth of the Belluno Basin can be referred to the Triassic–Jurassic boundary interval  
44  
45 175 or even to the latest Triassic. Above the Soverzene Formation, the Early Toarcian oceanic anoxic event  
46  
47 176 (Jenkyns, 1988) is recorded by discontinuous levels of black shales and manganoan carbonates,  
48  
49 177 contained within the Igne Formation, which consists of decimetric rhythms of grey marls and marly  
50  
51 178 mudstones (Jenkyns *et al.*, 1985; Claps *et al.*, 1995; Bellanca *et al.*, 1999). This last unit is covered by  
52  
53 179 the Vajont Limestone, composed of oolitic sands and biogenic skeletal debris redeposited by means of  
54  
55 180 gravity-flow processes that transferred oolitic sands from the western edge of the Friuli Platform into

1  
2  
3 181 slope and basin environments (Bosellini and Masetti, 1972; Bosellini *et al.*, 1981). The age of the  
4  
5 182 Vajont Limestone has been revised by Cobianchi (2002), by means of nannofossil biostratigraphy  
6  
7 183 performed on several sections, and can be ascribed to the late Bajocian–Bathonian interval. The  
8  
9 184 Fonzaso Formation (Callovian to Lower Kimmeridgian) overlies the Vajont Limestone and consists of  
10  
11 185 pelagic cherty mudstones and skeletal-rich turbidites and debris-flow deposits. The Fonzaso Formation  
12  
13 186 grades upwards into nodular, micritic red limestones very similar to the Rosso Ammonitico Veronese  
14  
15 187 (Upper Member, Upper Kimmeridgian to Lower Tithonian; Martire, 2007).

### 18 189 **2.3. The Friuli Platform**

20  
21 189 In a similar way to the Trento Platform, Masetti *et al.* (2012) proposed a further subdivision of the Friuli  
22  
23 190 Platform into a northern and a southern area (Figs 2 and 3). The northern area is characterized by a  
24  
25 191 stratigraphic evolution similar to that experienced by the eastern and northern sector of the Trento  
26  
27 192 Platform, in which the shallow-water Rotzo Formation is missing and the Monte Zugna Formation is  
28  
29 193 overlain by the Fanes Piccola Encrinite. On top of this last unit lies a deep-water, Middle and Upper  
30  
31 194 Jurassic succession, typical of the Belluno Basin (Vajont Limestone and Fonzaso Formation). To the  
32  
33 195 south, the classic persistent carbonate platform is exemplified by the section cropping out along the  
34  
35 196 Valcellina Valley, located at the southern edge of the Friuli Prealps, in which the exposed shallow-water  
36  
37 197 succession spans the interval from the Oxfordian through the whole of the Cretaceous (Cuvillier *et al.*,  
38  
39 198 1968).

40  
41 199 Bearing in mind the above-mentioned stratigraphic setting shown in Fig. 2, four stratigraphic sections  
42  
43 200 have been selected, each being representative of the different sectors in which Masetti *et al.* (2012)  
44  
45 201 subdivided the main palaeogeographic units of the Eastern Southern Alps. These sections allowed the  
46  
47 202 generation of a chemostratigraphic transect across the whole domain of the Eastern Southern Alps,  
48  
49 203 from the Garda Lake up to the eastern Italian border (Fig. 2).

### 50 204 **3. CHEMOSTRATIGRAPHIC TRANSECT ACROSS THE EASTERN SOUTHERN ALPS**



1  
2  
3 205 The stratigraphic sections selected are, from east to west (Figs 2 and 3): Monte Verzegnis, located in  
4  
5 206 the Belluno Basin; Monte Cumieli, located in the northern sector of the Friuli Platform; Foza, in which  
6  
7 207 the Rotzo Formation is missing and the Middle Jurassic Rosso Ammonitico rests directly on top of the  
8  
9 208 Monte Zugna Formation; and Chizzola, representative of the central-western area of the Trento  
10  
11 209 Platform (with the Pliensbachian Rotzo Formation). In all these sections, chemostratigraphic sampling  
12  
13 210 has been concentrated just below the unconformity surface at the top of the shallow-water succession  
14  
15 211 where distinctive carbon-isotope anomalies were predicted to be present (Fig. 3).

### 212 **3.1 Chemostratigraphic sampling and analyses**

#### 213 *Analytical techniques*

214 Chemostratigraphic sampling was performed on the selected stratigraphic sections at a resolution of  
215 20 cm, wherever allowed by the exposure conditions; powdered samples were obtained directly by  
216 means of a drill powered by a generator with micritic matrix being preferentially sampled and skeletal  
217 fragments and veins being avoided, on the assumption that these components would be more prone to  
218 vital effects and diagenesis. The high-resolution sampling preceded lower resolution sampling (a  
219 sample every 2 metres) in order to identify the main isotopic anomalies occurring in the section. The  
220 total thickness of the stratigraphic succession, corresponding to the 4 sections presented here, on  
221 which this high-resolution sampling has been performed, exceeds 570 m. For isotopic analysis, the  
222 samples were analysed isotopically for  $\delta^{13}\text{C}$  and  $\delta^{18}\text{O}$  using a VG Isogas Prism II mass spectrometer  
223 with an on-line VG Isocarb common acid bath preparation system. Samples were cleaned with  
224 hydrogen peroxide ( $\text{H}_2\text{O}_2$ ) and acetone [ $(\text{CH}_3)_2\text{CO}$ ] and dried at  $60^\circ\text{C}$  for at least 30 minutes. In the  
225 instrument they were reacted with purified phosphoric acid ( $\text{H}_3\text{PO}_4$ ) at  $90^\circ\text{C}$ . Calibration to PDB  
226 standard via NBS-19 was made daily using the Oxford in-house (NOCZ) Carrara marble standard.  
227 Reproducibility of replicated standards was typically better than 0.1‰ for both  $\delta^{13}\text{C}$  and  $\delta^{18}\text{O}$ .  
228 For strontium-isotope analyses, approximately 50 mg carbonate per sample were dissolved in 6 ml of  
229  $2\text{HNO}_3$  for both  $^{87}\text{Sr}/^{86}\text{Sr}$  and trace-metal analyses. A 1.5-mL aliquot of the dissolved solution was  
230 taken to perform strontium purification for the  $^{87}\text{Sr}/^{86}\text{Sr}$  measurements, and the remaining solution was

1  
2  
3 231 diluted and measured for Sr, Mn and Fe concentrations. Strontium was separated by a standard  
4  
5 232 chromatography method using Eichrom Sr resin, and the purified solution was dried at 100 °C and  
6  
7 233 re-dissolved in 2% HNO<sub>3</sub> prior to the isotopic analysis. The total blank was < 2 ng Sr. The <sup>87</sup>Sr/<sup>86</sup>Sr  
8  
9 234 measurements were performed on a Nu Plasma multi-collector inductively coupled plasma mass  
10  
11 235 spectrometer (Plasma 1), and the trace-metal abundances were measured on a Thermo-Finnigan  
12  
13 236 inductively coupled plasma mass spectrometer (Element II) at the University of Oxford. Both  
14  
15 237 instruments were coupled with a membrane desolvating system (Aridus, Cetac) to achieve high signal  
16  
17 238 sensitivity and stability. For <sup>87</sup>Sr/<sup>86</sup>Sr measurements, all isotopes (<sup>88</sup>Sr, <sup>87</sup>Sr, <sup>86</sup>Sr, <sup>85</sup>Rb, <sup>84</sup>Sr and <sup>83</sup>Kr)  
18  
19 239 were measured in static mode. To achieve maximum precision and accuracy, the <sup>88</sup>Sr signal was kept  
20  
21 240 between 13 and 16 V, and a minimum of 40 isotope ratios were collected with 20-second integration  
22  
23 241 time per ratio. <sup>83</sup>Kr was monitored to correct for the interference of <sup>86</sup>Kr on <sup>86</sup>Sr, and likewise <sup>85</sup>Rb was  
24  
25 242 monitored for <sup>87</sup>Rb correction on <sup>87</sup>Sr. <sup>83</sup>Kr intensity was generally consistent and below 0.2 mV, and  
26  
27 243 <sup>85</sup>Rb varied between samples but was generally lower than 2 mV. Samples were measured using a  
28  
29 244 standard bracketing method with the NIST SRM 987 standard. The instrument mass fractionation was  
30  
31 245 corrected internally using <sup>86</sup>Sr/<sup>88</sup>Sr = 0.1194. The external reproducibility of <sup>87</sup>Sr/<sup>86</sup>Sr in SRM 987  
32  
33 246 showed a value of 0.710258 ± 0.000049 (2 S.D.) from August to September, 2013.

#### 34 35 36 37 38 247 *Diagenesis versus palaeoceanography*

39  
40 248 The diagenetic behaviour of carbon and oxygen isotopes in shallow-water carbonates is problematic  
41  
42 249 because such materials are particularly susceptible to meteoric-water diagenesis. Such facies  
43  
44 250 accumulate close to sea level, small changes in which can lead to periodic emergence. The resultant  
45  
46 251 diagenesis would typically introduce fluids with relatively low δ<sup>18</sup>O and δ<sup>13</sup>C values derived from  
47  
48 252 rainwater after its interaction with atmospheric carbon dioxide and humus-rich soils (Hudson, 1977;  
49  
50 253 Marshall, 1992). Typically, horizons affected by such processes would have scattered and relatively low  
51  
52 254 carbon- and oxygen-isotope ratios compared to typical marine values. Other possible causes for  
53  
54 255 deviation of isotopic values from primary signals include variable quantities of skeletal grains exhibiting  
55  
56 256 non-equilibrium fractionation, different quantities of aragonite and calcite in the original sediment  
57  
58  
59  
60

1  
2  
3 257 (Swart, 2008), and the presence of void-filling secondary, low-Mg calcite in cavities opened in the  
4  
5 258 supratidal environment (e.g. Grötsch *et al.*, 1998; Davey and Jenkyns, 1999). Despite the possible  
6  
7 259 modification of shallow-water carbonates introduced by meteoric-water diagenesis, the primary  
8  
9 260 isotopic signal of carbon should not change substantially because the amount of carbon in diagenetic  
10  
11 261 fluids is low, unlike the case with oxygen, whose primary isotopic signal can also be deeply modified  
12  
13 262 during burial with recrystallization at relatively high temperatures (Scholle and Arthur, 1980). If  
14  
15 263 chemostratigraphic analysis is simultaneously performed on the same stratigraphic interval in both  
16  
17 264 shallow- and deep-water Jurassic successions, in conjunction with available biostratigraphy  
18  
19 265 (calcareous algae and benthonic foraminifera in platform carbonates and ammonites in deep-marine  
20  
21 266 carbonates), the presence of similar carbon-isotope anomalies in all sections proves the primary nature  
22  
23 267 of these major oceanographic and carbon-cycle perturbations (Woodfine *et al.*, 2008; Trecalli *et al.*,  
24  
25 268 2012; Sabatino *et al.*, 2013).

### 269 **3.2 The Monte Verzegnis section**

270 This section, 260 m thick (Fig. 4), has been measured and sampled in the homonymous mountain  
271 group located in the Carnian Alps, not far from the small town of Tolmezzo. The section contains little  
272 dolomite. From the palaeogeographic point of view, it belongs to the north-eastern sector of the Belluno  
273 Basin (Fig. 2).

#### 274 *Lithostratigraphy.*

275 The Lower Jurassic fill of the Belluno Basin is made of thin-bedded, cherty mudstones and  
276 wackestones with peloids, radiolarians and sponge spicules representing the Soverzene Formation  
277 (Fig. 4). This unit has been interpreted as peri-platform ooze (cf., Schlager and James, 1978) in which  
278 pelagic material falling through the water column has mixed with the carbonate mud supplied from  
279 adjacent carbonate platforms (Zanferrari *et al.* 2013). The Soverzene Fm. is about 200 m thick and lies  
280 atop the peritidal deposits of the Dachstein Limestone containing Upper Triassic megalodontids and  
281 the foraminifer *Triasina hantkeni*, thus allowing the time of the initial development of the Belluno Basin  
282 to be fixed as close to the Triassic–Jurassic boundary. In its uppermost portion, corresponding to a

1  
2  
3 283 thickness of 16 m (Fig. 4), the Soverzene Fm. is enriched in white chert that forms thick bands (up to 40  
4  
5 284 cm) interbedded with thinner limestones. The rise in the silica content corresponds to an increase of the  
6  
7 285 proportion of sponge spicules in the rock, likely indicative of the onset of mesotrophic conditions in the  
8  
9 286 Belluno Basin (cf., Föllmi *et al.*, 1994).

10  
11 287 The Soverzene Fm. passes upward, through an unconformable boundary, to a bi-directional  
12  
13 288 cross-bedded calcarenitic unit, 20 m thick, present at the top of this Formation in the whole area of the  
14  
15 289 Carnian and Julian Prealps. This unit is composed of grainstones with small superficial ooids in which  
16  
17 290 radiolarians and sponge spicules are mixed with benthic foraminifera and crinoidal fragments,  
18  
19 291 recording an ephemeral shallowing-upward evolution experienced during this time by the Carnian  
20  
21 292 Prealps area of the Belluno Basin (Zanferrari *et al.*, 2013). This calcarenitic unit of the Soverzene Fm. is  
22  
23 293 truncated by a hardground surface coated with Fe-Mn oxyhydroxide crusts, on top of which lies the  
24  
25 294 Mount Verzegnis Encrinite, a condensed unit, about 20 m thick, characterized by the intercalation of  
26  
27 295 cross-bedded, red crinoidal calcarenites and red nodular limestones in facies of the Lower Rosso  
28  
29 296 Ammonitico, commonly showing peculiar stromatolitic/thrombolitic structures similar to those described  
30  
31 297 by Jenkyns (1971) from western Sicily and Massari (1981) from the Trento Plateau. Further upward,  
32  
33 298 this unit passes into the Vajont Limestone, largely constituted by redeposited oolitic grainstones,  
34  
35 299 recording a return to basinal conditions on top of the underlying shallower water deposits.

#### 300 *Biostratigraphy*

301 The Soverzene Fm. is referred in the literature to the Hettangian–Pliensbachian (Zanferrari *et al.* 2013).  
302 During the measuring of the section, a specimen of an ammonite, which has been identified by F.  
303 Venturi (Perugia University) as pertaining to the genus *Arnioceras*, was discovered in a debris cone fed  
304 from a small cliff located about forty metres below the top of the Soverzene Fm. The *Arnioceras* genus  
305 has a distribution that embraces the *semicostatum*, *turneri*, *obtusum* and, possibly, *oxynotum*  
306 ammonite zones (transition from the early to the late Sinemurian; Dommergues *et al.*, 1994, Fig. 5),  
307 here informally called “Arnioceras time”. The finding of the *Arnioceras* 20 metres below the top of the  
308 unit indicates deposition of the main part of the Soverzene Formation, at least in this part of the Belluno

1  
2  
3 309 Basin, during the Hettangian–Sinemurian interval. The crinoid-rich calcarenitic unit at the top of the  
4  
5 310 Soverzene Fm. is devoid of ammonites and nannofossils (Erba, 2011, personal communication); a  
6  
7 311  $^{87}\text{Sr}/^{86}\text{Sr}$  ratio from a belemnite rostrum collected a few centimetres below its upper boundary gave a  
8  
9 312 value of  $0.707196 \pm 0.000042$  (normalized against a value of 0.710250 for the NBS-987 standard)  
10  
11 313 suggesting an age interval either spanning the mid-Pliensbachian to the Early Toarcian or the Early  
12  
13 314 Bajocian (reference curve in Jones *et al.* 1994; Jenkyns *et al.*, 2002). This evidence suggests that this  
14  
15 315 unit could be considered the more open-marine counterpart of the mid-upper portion of the Rotzo Fm.  
16  
17 316 in the Venetian Prealps and could be ascribed to the Pliensbachian p.p. (Masetti *et al.* 1998; Posenato  
18  
19 317 and Masetti, 2012).  
20  
21  
22 318 In the Monte Verzegnis Encrinite, referred in the literature to the Toarcian p.p.–Bajocian p.p. (Piano and  
23  
24 319 Carulli, 2002) some ammonite specimens have been collected in the lower part of the formation.  
25  
26 320 Among these, G. Pavia (Turin University) determined *Teloceras cf. triptolemus* (Buckman) and  
27  
28 321 *Holophilloceras sp.* ammonites, both referable to the Early Bajocian. A  $^{87}\text{Sr}/^{86}\text{Sr}$  determination of a  
29  
30 322 belemnite collected in the lowermost part of the Verzegnis Encrinite, gave a value of  $0.707062 \pm$   
31  
32 323  $0.000042$  (normalized against a value of 0.710250 for the NBS-987 standard) indicating either the  
33  
34 324 Pliensbachian–Toarcian boundary or a time interval spanning from the Early Bajocian to the Early  
35  
36 325 Bathonian. Taken together, the data confirm an Early Bajocian age of the lower portion of the unit. No  
37  
38 326 ammonites have been found in the upper part of the Monte Verzegnis Encrinite and, by analogy with  
39  
40 327 the similar Rosso Ammonitico cropping out in other areas of the eastern Southern Alps (Martire, 2007),  
41  
42 328 it likely corresponds to the Bathonian–Early Callovian.  
43  
44  
45 329 In summary, the original biostratigraphic data suggest:  
46  
47 330 - in the Verzegnis section, the deep-water micritic unit of Soverzene Fm., chert-rich unit included,  
48  
49 331 corresponds to peri-platform ooze delivered to the basin during Hettangian–Sinemurian p.p. time, up to  
50  
51 332 and including the so-called “Arnioceras time”;  
52  
53  
54 333 -  $^{87}\text{Sr}/^{86}\text{Sr}$  data suggest that the calcarenitic unit at the top of the Soverzene Fm. belongs to the mid–  
55  
56 334 Late Pliensbachian, and it corresponds to the mid-upper portion of the Rotzo Fm. in the Venetian  
57  
58  
59  
60

1  
2  
3 335 Prealps, overlying the lower part of the same formation with a hiatus corresponding to the Late  
4  
5 336 Sinemurian–Early Pliensbachian; and the Verzegnis Encrinite was deposited during the Early  
6  
7 337 Bajocian–Early Callovian and lies unconformably on top of the Soverzene Formation with a hiatus  
8  
9 338 corresponding to the Toarcian–Aalenian interval.

### 11 339 *The $\delta^{13}C$ curve*

12  
13  
14 340 444 samples have been analyzed coming from a stratigraphic section 261-m thick (Fig. 4). The  
15  
16 341 high-resolution interval (20 cm/sample) goes from 146 to 240 m. The remaining under- and overlying  
17  
18 342 segments have been sampled with lower resolution (2 m/sample). Through the entire section, the  
19  
20 343 carbon-isotope values mostly fluctuate between  $\sim 1.5\text{‰}$  and  $\sim 3.5\text{‰}$ . In the lowest 60 m, the curve  
21  
22 344 mostly ranges between  $\sim 2\text{‰}$  and  $\sim 2.7\text{‰}$ : the relatively low resolution of the profile prevents reliable  
23  
24 345 identification of the negative peaks located at the T/J boundary. Stratigraphically higher, between 60  
25  
26 346 and 80 metres, including an unexposed interval of  $\sim 11$  m, the curve shifts towards consistent values  
27  
28 347 around  $2.5\text{‰}$ . Up to about 160 m, the curve fluctuates around a value of  $2.5\text{‰}$ , with a pronounced  
29  
30 348 positive shift (to  $\sim 3\text{‰}$  around 114 m). A small ( $0.5\text{‰}$ ) negative followed by a small ( $0.5\text{‰}$ ) positive  
31  
32 349 excursion characterizes the interval 140–160m. From here on up, the profile describes a symmetrical  
33  
34 350 oscillation that arrives at a minimum of  $\sim 1.4\text{‰}$  at  $\sim 196$  m then rises up to  $\sim 3.6\text{‰}$  at  $\sim 236$  m. This  
35  
36 351 spectacular and symmetric oscillation of the carbon-isotope curve corresponds to about 60 m of  
37  
38 352 section and is completely contained within the Soverzene Formation. The lowest value is located close  
39  
40 353 to the cliff where the *Arnioceras* specimen was found, just at the base of the chert-rich unit located at  
41  
42 354 the top of the typical micritic facies of the Soverzene Fm. At  $\sim 237$ – $238$  m the carbon-isotope curve  
43  
44 355 moves relatively abruptly to lower values ( $\sim 2.6\text{‰}$ ) just below the unconformable boundary between the  
45  
46 356 calcarenitic unit of the Soverzene Fm. and the Monte Verzegnis Encrinite before rising to  $>3.5\text{‰}$  at the  
47  
48 357 base of this latter unit.

### 53 358 **3.3 The Monte Cumieli section**

54  
55  
56 359 The Monte Cumieli section (Fig. 4) crops out in the Carnian Prealps, not far from the small town of  
57  
58 360 Gemona, is 126 m thick, and exemplifies the Jurassic succession of the northern sector of the Friuli

1  
2  
3 361 Platform, characterized by the early demise of the Early Jurassic carbonate platform of the Monte  
4  
5 362 Zugna Formation (Fig. 2) and by the lack of shallow-water carbonates younger than Sinemurian  
6  
7 363 (Zanferrari *et al.*, 2013).

8  
9  
10 364 *Lithostratigraphy.*

11 365 The Monte Zugna Formation is further subdivided, as illustrated in Fig. 4, into a lower peritidal and an  
12  
13 366 upper calcarenitic unit. The lower unit is 87 m thick and is composed of peritidal cycles representing the  
14  
15 367 Jurassic continuation of the depositional theme of the underlying, Upper Triassic Dolomia Principale.

16 368 The calcarenitic unit is 33 m thick and comprises metre-scale beds of oolitic grainstones that  
17  
18 369 become progressively richer upwards in echinoderm debris suggesting increasing open-marine  
19  
20 370 influence (e.g., Jenkyns, 1971). This calcarenitic body is interpreted as a subtidal shoal largely  
21  
22 371 controlled by storm waves whose activity is recorded by plane parallel lamination. Throughout the  
23  
24 372 entire unit, the ooids exhibit some degree of concentric structure; however, in the lower part of the unit,  
25  
26 373 the cortex is dominantly micritic, in some cases with outer thinly laminated tangential oriented crystals  
27  
28 374 (Fig. 6a). These micritic ooids are associated with oncoids, dasyclad algae (*Palaedasycladus*  
29  
30 375 *mediterraneus*, *Palaedasycladus gracilis*), and foraminifers (*Aeolisaccus dunningtoni*, *Siphovalvulina*  
31  
32 376 spp., *Everticyclammina praevirguliana*). The micritic ooids are replaced up-section by radial-fibrous  
33  
34 377 ooids whose structure is interrupted by dark microborings (Fig. 6b). The palaeontological assemblage  
35  
36 378 associated with these radial-fibrous ooids is characterized by foraminifera with a complex wall  
37  
38 379 structure (*Palaeomayncina termieri*, *Tersella genotii*, *Rectocyclammina* sp.), locally acting as nuclei for  
39  
40 380 the oolitic cortex (*Everticyclammina praevirguliana*, Fig. 6b).

41  
42 381 The Monte Zugna Formation is truncated by a disconformity surface on top of which lie the  
43  
44 382 cross-bedded crinoidal calcarenites of the Fanes Encrinite interpreted as sand-waves (Zanferrari *et al.*,  
45  
46 383 2013). Resedimented deposits of the Vajont Limestone represent the youngest unit cropping out in the  
47  
48 384 Monte Cumieli Section and record a deepening-upward evolution of the northern sector of the Friuli  
49  
50 385 Platform which, during the Middle Jurassic, foundered to become effectively part of the Belluno Basin  
51  
52  
53  
54  
55  
56  
57  
58  
59  
60

1  
2  
3 386 where it received oolitic turbidites derived from the southern portion of the same platform that persisted  
4  
5 387 as a productive shallow-water carbonate source (Masetti *et al.* 2012; Zanferrari *et al.*, 2013).  
6

7 388 *Biostratigraphy*  
8

9  
10 389 The shallow-water assemblage recorded in the Monte Cumieli section accords with the classic  
11  
12 390 successions of the Alpine-mediterranean Tethys as documented in the Central Apennines and  
13  
14 391 Southern Apennines by De Castro (1991), Chiocchini *et al.*, 1994, 2008), Western Croatia (Velić, 2007)  
15  
16 392 and Morocco (Septfontaine 1984; 1985). Barattolo and Romano (2005) recognize the following four  
17  
18 393 shallow-water carbonate-platform assemblages as pertaining to the Upper Triassic–Lower Jurassic:  
19  
20 394 1) Algal and foraminiferal Triassic assemblage (TA assemblage, uppermost Rhaetian) characterized by  
21  
22 395 the occurrence of dasycladaleans, *Griphoporella curvata* (Gümbel) and *Gyroporella vesiculifera*  
23  
24 396 Gümbel, involutinid foraminifera (essentially *Aulotortus* and *Triasina*) and oncoids. Macrofauna is  
25  
26 397 composed of the large shells of megalodontid bivalves. Foraminifera and megalodontids become more  
27  
28 398 common up-section, whereas dasycladaleans become rare or are missing altogether.  
29  
30

31 399 2) *Thaumatoporella* and *Aeolisaccus dunningtoni* assemblage (LA assemblage, lowermost  
32  
33 400 Hettangian–upper Hettangian) characterized by the exclusive occurrence of *Thaumatoporella* and  
34  
35 401 *Aeolisaccus dunningtoni* Elliott, mainly in the lower part of its range. Small siphonous valvulinid  
36  
37 402 foraminifera are rather rare, but up-section they become more common. Rare gastropods, bivalves and  
38  
39 403 corals may also occur. Oncolitic coatings on grains are common.  
40  
41

42 404 3) Lower Jurassic dasycladalean assemblage (LB assemblage, upper Hettangian–upper Sinemurian)  
43  
44 405 characterized by the occurrence of a variety of Liassic species of dasycladaleans. The most  
45  
46 406 representative genera are *Palaeodasycladus*, *Fanesella*, *Sestrosphera* and *Tersella*. Taxa of the  
47  
48 407 previous LA assemblage continue into the base of the LB assemblage, which can be subdivided into  
49  
50 408 lower (LB1) and upper (LB2) sub-assemblages. In LB1, Liassic dasycladaleans are not abundant and  
51  
52 409 LA microfossils are still important. In LB2, dasycladaleans become dominant and large foraminifera  
53  
54 410 appear (e.g. *Paleomayncina*).  
55  
56  
57  
58  
59  
60



1  
2  
3 411 4) Large foraminifer assemblage (LC assemblage, upper Sinemurian–Upper Plienbachian) marked by  
4  
5 412 a dominance of dasycladaleans, but with a relatively low diversity. Larger foraminifera with a complex  
6  
7 413 internal skeleton are abundant, the most widespread genera being *Orbitopsella*, *Lituosepta*, *Amijiella*  
8  
9 414 and *Haurania*. The background fauna is always composed of an LA assemblage.  
10  
11 415 The Monte Zugna Formation in the Monte Cumieli section is dominated by foraminifers (*Aeolisaccus*  
12  
13 416 *dunningtoni*, *Siphovalvulina* spp., *Meandrovoluta asiagoensis*, *Everticyclammina praevirguliana*) and  
14  
15 417 algae (*Thaumatoporella parvovesciculifera*, *Palaeodasycladus mediterraneus*, *Palaeodasycladus*  
16  
17 418 *gracilis*, *Tersella genotii* and *Cayeuxia*-like briopsidales); the calcarenitic unit records the first  
18  
19 419 occurrence of *Paleomayncina termieri* and an enrichment of foraminifera with a complex wall structure.  
20  
21 420 According to Zanferrari *et al.* (2013), the Monte Zugna Formation has been assigned a generic  
22  
23 421 Hettangian–Sinemurian age; the micropalaeontological content of the section corresponds to the upper  
24  
25 422 part of the LB1 and the lower part of the LB2 assemblages *sensu* Barattolo & Romano (2005).  
26  
27 423 The palaeontological assemblage of the overlying Fanes Piccola Encrinite is characterized by the  
28  
29 424 dominance of foraminifers (*Involutina liassica*, *Agerella martana*, *Lenticulina*, Frondicularia,  
30  
31 425 *Ophtalmididae* e *Nodosaridae*) of little reliable stratigraphic significance. Zanferrari *et al.* (2013)  
32  
33 426 interpreted this unit as the result of discrete, and virtually instantaneous, deposition of sand-waves  
34  
35 427 bounded by long-lasting periods of non-deposition that overall occurred between the age of the earliest  
36  
37 428 (“Arnioceras time”) and the age (Bajocian–Bathonian), of the base of the overlying Vajont Limestone).  
38  
39  
40  
41  
42  
43  
44

#### 430 *The $\delta^{13}C$ curve of the Monte Cumieli section*

431 274 samples have been analyzed from a 137-m-thick stratigraphic section (Fig. 4). The first segment of  
42  
43 432 the section, 55 m thick, has been sampled at relatively low resolution (2 m/sample), the second, 47.5 m  
44  
45 433 thick, extending up to the top, at higher resolution (one sample every 20 cm). Within the section, the  
46  
47 434 carbon-isotope values fluctuate between ~ 2.9‰ (90 m) and ~ 0.4‰ (107 m). Up to 43 m from the base,  
48  
49 435 within the peritidal unit of the Monte Zugna Formation, the profile evolves vertically with symmetric  
50  
51 436 oscillations centred around a value of 2‰. Higher in the stratigraphy, extending up to about 90 m, the  
52  
53  
54  
55  
56  
57  
58  
59  
60

1  
2  
3 437 curve moves to generally more positive values (maximum value in the section: 3‰) with a trend  
4  
5 438 interrupted by a couple of negative shifts (at 67 m and 84 m). This positive fluctuation of the curve  
6  
7 439 corresponds, on the base of the chemostratigraphic correlation (Figs 7, 8), to the upper part of the  
8  
9 440 peritidal unit and to the first few metres of the calcarenitic unit of the Monte Zugna Fm., recorded by a  
10  
11 441 thin intercalation of micritic deposits corresponding to the *Gervillia* beds of the Foza and Chizzola  
12  
13 442 sections. The calcarenitic unit, starting from the first occurrence of *Paleomayncina termieri*, records a  
14  
15 443 clear negative excursion in which values shift from ~ 2.9‰ (at ~ 90 m) to ~ 0.4‰ (at ~ 107 m); higher in  
16  
17 444 the section, the curve returns towards more positive values (~ 1.7‰) up to ~ 120 m, at the level of the  
18  
19 445 unconformity between the Monte Zugna Fm. and the Fanes Piccola Encrinite.  
20  
21

### 22 446 **3.4 The Foza section**

23  
24 447 The Foza section (Fig. 7) is located in the eastern sector of the Asiago Plateau (Venetian Prealps), is  
25  
26 448 73 m thick, and has been sampled along the road connecting the small towns of Valstagna, located in  
27  
28 449 Valsugana, to Foza, just below this last village. The Foza section exemplifies the Jurassic succession  
29  
30 450 of the north-eastern area of the Trento Plaform, characterized by the lack of Pliensbachian  
31  
32 451 shallow-water carbonates (Rotzo Formation) and hence early demise of the Early Jurassic carbonate  
33  
34 452 platform of the Monte Zugna Formation (Fig. 2 and 3).  
35  
36 453 *Lithostratigraphy.* The Foza section has been entirely sampled inside the Monte Zugna Fm, up to its  
37  
38 454 upper boundary with the Lower Rosso Ammonitico; in the shallow-water carbonates of the Monte  
39  
40 455 Zugna Fm. the peritidal features are less marked than elsewhere, but the depositional environment  
41  
42 456 may be interpreted as the internal, slack-water and muddy sector of the carbonate platform (Romano *et*  
43  
44 457 *al.* 2005). As with the Monte Cumieli section, a calcarenitic unit, 33 m thick, is superimposed on the  
45  
46 458 lower, mainly micritic unit of the formation (Fig. 7); this granular unit is split into two parts by intercalated  
47  
48 459 fine-grained deposits of lagoonal character containing the bivalve *Gervillia buchi* (Fig. 7). Here the  
49  
50 460 ooids also exhibit a stratigraphic evolution in which the micrite-coated grains with thinly laminated  
51  
52 461 tangential cortices (Fig. 6a), present at the base, are replaced up-section by radial-fibrous ooids (Fig.  
53  
54 462 6b).  
55  
56  
57  
58  
59  
60

463 *Biostratigraphy*

464 The micropalaeontological content is similar to that present in the Monte Cumieli section. The micritic  
465 unit is characterized by dasycladaleans (*Palaedasycladus mediterraneus*, *Sestrosphaera liasina* and  
466 *Eodasycladus* sp.) and the foraminifer *Everticyclammina praevirguliana*. In addition to this, the  
467 calcarenitic unit contains *Palaomayncina termieri*, *Terquemella* sp (dasycladalean calcified  
468 reproductive organs) and the coprolite *Favreina* sp. The first occurrence of *Palaomayncina termieri*  
469 falls in the middle of the calcarenitic unit, about 20m below the unconformity. The Monte Zugna  
470 Formation has been assigned to the Hettangian–Sinemurian interval (Romano *et al.*, 2005). The  
471 micropalaeontological assemblage of the Foza section, like that of the Monte Cumieli section,  
472 corresponds to the upper part of the LB1 and the lower part of the LB2 assemblages *sensu* Barattolo &  
473 Romano (2005). The unconformity surface is covered by the Rosso Ammonitico Inferiore whose  
474 stratigraphical extent in the Trento Plateau is referred to the upper Bajocian–Lower Callovian (Martire,  
475 2007).

477 *The  $\delta^{13}C$  curve of the Foza section*

478 324 samples have been analyzed coming from a 70-m-thick stratigraphic section (Fig. 7). The  $\delta^{13}C$   
479 values, which are highly scattered, mostly fall between -2 and 2‰. Overall, the curve can be split into  
480 three minor negative excursions separated by positive rebounds. The stratigraphically lowest negative  
481 excursion corresponds to the 0–16 m segment of the section, reaches a minimum value of ~ -0.9‰ (at  
482 10.6 m) and returns to a value of ~ 2‰ (at 15.8 m); the second reaches ~ -2.40‰ at 32 m from the base  
483 (not shown in figure) then moves rather abruptly in a positive sense toward a value of 2.45‰ at the  
484 level of a bivalve bed (*Gervillia*) located at about 40m from the base of the section, close to the lower  
485 boundary of the calcarenitic unit of the Monte Zugna Formation. The third, relatively broad negative  
486 excursion starts from a value of ~ 2.5‰ (highest value in the section: 42.5 m), then falls abruptly,  
487 following the calcarenitic unit and the stratigraphical distribution of *Palaomayncina termieri*, to reach a  
488 minimum of ~ -1.4‰ (56 m) and returns to ~ 2.5‰ at the boundary with the Rosso Ammonitico,

### 489 3.5. The Chizzola section

490 This section (Fig. 7) represents the central-western areas of the Trento Platform (Fig. 2) in which the  
491 Pliensbachian shallow-water unit (Rotzo Fm.) lies on top of the Monte Zugna Formation. Located in the  
492 Adige Valley, the Chizzola section has been sampled along the road connecting the villages of Chizzola  
493 and Mori. The top of the section, corresponding to the upper half of the Loppio Oolitic Limestone, has  
494 been measured near Nomi village.

#### 495 *Lithostratigraphy*

496 The Chizzola section exposes the upper portion of the Monte Zugna Formation (92 m) and the whole  
497 thickness of the Loppio Oolitic Limestone (32 m). The first unit is further subdivided into a peritidal  
498 calcarenitic unit (25 m) in which the peritidal cycles are made of cross-bedded, subtidal oolitic  
499 calcarenites passing upwards in the cycle to inter-supratidal stromatolites, locally with dinosaur tracks  
500 (Avanzini *et al.* 1997), and an upper, subtidal, nodular unit (67 m) cut by a neptunian dyke filled with  
501 oolites derived from the overlying Loppio Oolitic Limestone. The occurrence of peritidal facies in the  
502 calcarenitic unit of the Monte Zugna Formation is a peculiar feature of the Adige Valley, and the  
503 sediments have been interpreted by Masetti *et al.* (1998) as deposited inside small tidal flats,  
504 developed behind marginal shoals, that were retrograding towards the inner part of the Trento Platform  
505 during a transgressive phase. The nodular subtidal units are interpreted as representing a deepening  
506 phase of the topmost portion of the Monte Zugna Fm., which is missing in the other sections; the Loppio  
507 Oolitic Limestone is an oolitic body interposed between the Monte Zugna Fm. and the Rotzo Fm. that  
508 spread across the main portion of the underlying unit during a sea-level rise that pushed the marginal  
509 oolitic bars composing this unit from west to east across the Trento Platform (Fig. 3; Masetti *et al.*  
510 1998).

#### 511 *Biostratigraphy*

512 The micropalaeontological content of the Monte Zugna Fm. is similar to that described in the two  
513 previous sections. As regards the Loppio Oolitic Limestone, the lack of fauna of significant value  
514 precludes reliable stratigraphic attribution and it is generically referred to the Sinemurian stage. The

1  
2  
3 515 stratigraphic setting of the Rotzo Formation is still matter of debate: either from the upper Sinemurian to  
4  
5 516 the upper Pliensbachian, if assigned on the base of foraminiferal biostratigraphy (Fugagnoli, 2004), or  
6  
7 517 from the lower Pliensbachian to the upper Pliensbachian, on the base of ammonite biostratigraphy  
8  
9 518 (Posenato and Masetti, 2012). The sharp bounding surface between the Loppio Oolitic Limestone and  
10  
11 519 the Rotzo Formation, locally encrusted with red ferruginous coatings, suggests that the contact  
12  
13 520 between these two units represents a regionally extensive unconformity.

### 16 521 *The $\delta^{13}\text{C}$ curve of the Chizzola section*

17  
18 522 508 samples have been analyzed from a 118-m-thick stratigraphic section (Fig. 7) with a sampling  
19  
20 523 resolution of 20 cm. The entire carbon-isotope curve fluctuates between values of  $\sim -1.6\text{‰}$  ( $\sim 4.5$  m)  
21  
22 524 and  $\sim 2.4\text{‰}$  ( $\sim 25$  m), with values being particularly scattered in the basal 20m. The curve illustrates a  
23  
24 525 positive excursion ( $\sim 2.4\text{‰}$ ) at 7.5 m, declining abruptly to a relative minimum at 13 m, before moving  
25  
26 526 again to more positive values that reach a maximum value of  $\sim 2.4\text{‰}$  at 25 m. These positive–negative  
27  
28 527 oscillations are entirely contained within the calcarenitic unit of the Monte Zugna Fm., here  
29  
30 528 characterized by peritidal features. Above these excursions and extending for about 60 m up to  $\sim 84$  m,  
31  
32 529 within the upper portion of the Monte Zugna Fm. in which peritidal structures are missing, the profile  
33  
34 530 displays another broad negative excursion, centred around the neptunian dyke and reaching the lowest  
35  
36 531 value of  $\sim 0.1\text{‰}$  at about 53 m: positive indentations are present around 35 m and 44 m. The top of the  
37  
38 532 subtidal, mainly micritic unit of the Monte Zugna Fm., from 84 to 92 m ( $\sim 1.6\text{‰}$ ), corresponds to a third  
39  
40 533 negative excursion (minimum value of  $\sim 0.8\text{‰}$  at 89 m) between two positive excursions. The curve  
41  
42 534 becomes more stable in the remaining part of the unit, fluctuating around an average value of about 1.3  
43  
44 535 ‰, with a minor positive excursion around 114 m.

### 49 536 **3.6 Correlations of $\delta^{13}\text{C}$ curve across the Eastern Southern Alps and their comparison with** 50 51 537 **coeval anomalies**

52  
53 538 The proposed correlation of the above-described anomalies of the  $\delta^{13}\text{C}$  curves across the entire  
54  
55 539 Eastern Southern Alps, from the Garda Lake to the eastern Italian border, is illustrated by the grey band  
56  
57 540 in Figure 8. The excellent matching between the single curves allows recognition, both in the shallow-

1  
2  
3 541 and deep–water units, of a distinct abrupt positive followed by broader negative carbon-isotope  
4  
5 542 excursion (CIE) located just below an unconformity surface (Fig. 3). The primary origin of these  
6  
7 543 excursions is supported by the following observations: all the coeval segments sampled in different  
8  
9 544 sections exhibit the same carbon-isotope excursions with similar geometry and extending over similar  
10  
11 545 stratigraphic thicknesses; all the curves are characterized by well-defined trends and not by single  
12  
13 546 peaks that might represent diagenetic artifacts; the curves conform with the stratigraphic occurrence of  
14  
15 547 key faunal datum levels; the curves conform with similar facies developments.

16  
17  
18 548 In the basinal Monte Verzegnis section, the carbon-isotope excursion spans a stratigraphic thickness of  
19  
20 549 about 60–70 m (depending on chosen baseline), referable, thanks to the finding of a specimen of  
21  
22 550 *Arnioceras*, to a time interval ranging from the base of the *semicostatum*, through the *turneri* to the top  
23  
24 551 of the *obtusum* Zones (Dommergues *et al.*, 1994, Fig. 5) and thus likely corresponding to an interval of  
25  
26 552 2–3 Ma (Gradstein *et al.*, 2012). The same negative CIE is clearly recognizable, with a similar  
27  
28 553 geometry, in the two palaeogeographic domains situated either side of the Belluno Basin, namely in the  
29  
30 554 Monte Cumieli section (Friuli Platform) and the Foza Section (northern sector of the Trento Platform).  
31  
32 555 Although values are scattered, this negative CIE signal, which is entirely contained within the  
33  
34 556 calcarenitic unit at the top of the Monte Zugna Formation (thickness around 30 m), is not only preceded  
35  
36 557 by a positive excursion but also interrupted by positive indentations. Significantly, the positive to  
37  
38 558 negative shift at the base of the major negative CIE correlates with the first occurrence of the  
39  
40 559 *Paleomayncina termieri* foraminifer in both the Foza and Monte Cumieli sections. The isotopic  
41  
42 560 correlation with strata containing *Arnioceras* allows this foraminifer, once attributed to a poorly defined  
43  
44 561 Sinemurian age, to be linked to the transition from the lower to the upper part of the stage. In the  
45  
46 562 Chizzola section, located on the other side of the Trento Platform, this negative CIE is contained within  
47  
48 563 the ~25 m-thick calcarenitic unit of the Monte Zugna Formation.

49  
50 564 Most Jurassic chemostratigraphical studies to date have been mainly focused on the Pliensbachian–  
51  
52 565 Toarcian interval; other stages are less well defined. In the Hettangian–Sinemurian interval, Jenkyns *et*  
53  
54 566 *al.* (2002) recorded carbon-isotope ratios from belemnites and oyster shells from Portugal and England

1  
2  
3 567 indicating a positive excursion in the Lower Sinemurian followed by a negative excursion at the  
4  
5 568 Sinemurian–Pliensbachian boundary. More detail is given by Jenkyns and Weedon (2013), who  
6  
7 569 illustrate a high-resolution organic-carbon isotope curve from Sinemurian black shales cropping out in  
8  
9 570 the Wessex Basin (Dorset, UK). These data show a negative excursion likely centred around the  
10  
11 571 boundary of the *semicostatum* and *turneri* Zones, a positive excursion extending through the upper  
12  
13 572 *turneri* Zone before a fall at the close of that zone into the lower part of the *obtusum* Zone, followed by  
14  
15 573 a rise before the continuity of the section is interrupted by a hiatus (Fig. 8). This positive *turneri*-Zone  
16  
17 574 excursion has been recorded also by Porter *et al.* (2014) in marine sediments from North America  
18  
19 575 (British Columbia, Canada) and manifestly represents a global marine carbon-isotope signature.  
20  
21 576 Riding *et al.* (2012) studied a section from a borehole in eastern England and documented a marked  
22  
23 577 negative excursion in a  $\delta^{13}\text{C}$  curve from wood and palynomorphs centred in the *oxynotum* Zone (lower  
24  
25 578 part of the Upper Sinemurian, Fig. 5), an interval that is missing in the Dorset profile. This negative  
26  
27 579 excursion, registered in both marine and terrestrial carbon (thereby indicating a response in both  
28  
29 580 atmosphere and oceans) was coupled with an increase in abundance of the thermophilic pollen  
30  
31 581 *Classopollis classoides* (Fig. 9), suggesting the occurrence of a warming event.  
32  
33  
34 582 In Morocco, carbonate isotopic data from Lower Jurassic peritidal platform carbonates show a  
35  
36 583 well-defined negative excursion attributed to the early Sinemurian and a positive excursion in overlying  
37  
38 584 open-marine sediments whose basal levels contain the ammonite *Arnioceras* and are placed in the late  
39  
40 585 Sinemurian (Wilmsen and Neuweiler, 2008). In England and other parts of northern Europe, *Arnioceras*  
41  
42 586 ranges from the *bucklandi* Zone of the basal Sinemurian into the *obtusum* Zone (Page, 2010), in good  
43  
44 587 correspondence with the distribution proposed by Dommergues *et al.* (2004; Fig. 5). If we take the  
45  
46 588 high-resolution data from all these sections as a guide (Figs 4, 6, 7), it seems that there are two  
47  
48 589 possible negative excursions over the likely stratigraphical range of *Arnioceras*. If we concentrate on  
49  
50 590 positive excursions, the most pronounced of which in the Dorset profile is in the upper part of the *turneri*  
51  
52 591 Zone (Fig. 9), then the suggested zonal equivalence in the Verzegnis profile is as suggested in Figure  
53  
54 592 8. A negative trend covers the interval attributed to the *semicostatum* and possibly some of the *turneri*  
55  
56  
57  
58  
59  
60

1  
2  
3 593 Zone, whose defining feature, however, is a positive excursion, albeit relatively small in the Verzegnis  
4  
5 594 profile. Following the *turneri*-Zone positive excursion, there is a well-defined negative excursion in the  
6  
7 595 *obtusum* Zone, likely extending into the *oxynotum* Zone, followed by near-symmetrical recovery to  
8  
9  
10 596 higher values: a pattern matching that in the borehole material in eastern England (Fig. 9). In the  
11  
12 597 platform-carbonate sections, the abrupt positive excursions seen in Chizzola, Foza and Monte Cumieli  
13  
14 598 can thus be referred to the *turneri* Zone and the ensuing negative excursion to the *obtusum* and  
15  
16 599 *oxynotum* Zones.

#### 600 4.0 POSSIBLE CAUSES OF THE “*ARNIOCERAS* TIME” NEGATIVE $\delta^{13}\text{C}$ EXCURSION

601 The “*Arnioceras* time” broad negative  $\delta^{13}\text{C}$  excursion of  $\sim 1.0\text{‰}$  recorded in the Soverzene Formation  
602 of the Monte Verzegnis section is well defined and extends over a thickness of  $\sim 60$  m. Unlike the  
603 negative excursion that characterizes the early Toarcian interval, which is abrupt with a clear stepped  
604 profile in all sections (Hesselbo *et al.*, 2007; Kemp *et al.*, 2005; Hermoso *et al.*, 2012; Jenkyns *et al.*,  
605 2002; Sabatino *et al.*, 2009), the excursion at Monte Verzegnis appears more gradual with values  
606 dropping from  $\sim 2.5\text{‰}$  to  $\sim 1.5\text{‰}$ . If values of  $\sim 2.5\text{‰}$ , which characterize the lower parts of the section,  
607 are taken as background, the negative shift may record introduction of isotopically light carbon into the  
608 ocean–atmosphere through oxidation of a formerly buried reservoir such as sub-seafloor clathrates or  
609 organic-rich sediments. Alternatively, a reduction in the amount of global biomass or organic carbon  
610 buried in response to environmental change could have caused movement to lower carbon-isotope  
611 values. LIP volcanism cannot be invoked, because there are no known provinces of this age (Courtillot  
612 and Renne, 2003): the main activity phase of the Central Atlantic Magmatic Province (CAMP) occurred  
613 around 200 Ma and terminated during Hettangian time (Marzoli *et al.*, 1999).

614 If isotopically light  $\text{CO}_2$  were to have been introduced into the atmosphere, resultant global warming  
615 would have likely led in turn to acceleration of the hydrological cycle and to the increase of global  
616 weathering rates. Increased quantities of nutrients and fine-grained continental sediments delivered to  
617 oceans would have favoured both increased organic productivity and formation of salinity-stratified  
618 water bodies leading to the onset of eutrophic conditions and deposition of organic-rich clays and



1  
2  
3 619 clay-rich limestones. No such markers of wet and humid conditions during the CIE have been so far  
4  
5 620 identified in the Southern Alps during “*Arnioceras* Time”, but a coeval warming event has been  
6  
7 621 recognized in Southern England by Riding *et al.* (2012), based on palynological data and extending  
8  
9 622 over the *obtusum* and *oxynotum* Zones (Fig. 9). A possible important role in the release of the  
10  
11 623 isotopically light  $^{12}\text{C}$  into the atmosphere could have been played by syn-sedimentary tectonics that  
12  
13 624 caused fracturing and leakage of gas-hydrate reservoirs (cf., Jenkyns, 2010). The negative excursion of  
14  
15 625 “*Arnioceras* time” occurred coincidentally with the reactivation of the rifting activity that affected large sectors  
16  
17 626 of the Tethyan areas from the Southern Alps, Apennines and Sicily to the Betic Cordillera (Spain) and  
18  
19 627 Moroccan High Atlas (Masetti *et al.*, 1998; Marino and Santantonio, 2010; Ruiz Ortiz *et al.*, 2004; Merino  
20  
21 628 Tomé *et al.*; 2012). This coincidence in timing could explain why many authors have ascribed local to  
22  
23 629 regional drowning of carbonate platforms primarily to tectonic causes affecting subsidence rate rather than  
24  
25 630 climatic influence on the sediment factory itself.  
26  
27  
28  
29  
30  
31

### 32 632 **5.0 IMPACT OF THE “*ARNIOCERAS* TIME” NEGATIVE $\delta^{13}\text{C}$ EXCURSION ON CARBONATE SEDIMENTATION**

33  
34 633 The inferred position of the “*Arnioceras* Time” negative  $\delta^{13}\text{C}$  excursion within the Lower Jurassic  
35  
36 634 succession along the transect crossing the Eastern Southern Alps is shown in Figures 3 and 8. In the  
37  
38 635 Belluno Basin, the negative carbon-isotope anomaly corresponds with the upper part of the lower  
39  
40 636 micritic unit of the Soverzene Fm., with the lowest values located just below the base of the chert-rich  
41  
42 637 unit at the top of the same formation (Figs 4, 7 and 8). In the shallow-water carbonates, both in the  
43  
44 638 Trento and Friuli platforms, the anomaly begins at the top of the lower, peritidal unit of the Monte Zugna  
45  
46 639 Fm., is interrupted by a short positive  $\delta^{13}\text{C}$  pulse, and culminates in the calcarenitic unit at the top of the  
47  
48 640 same Formation.  
49  
50

51  
52 641 The chert-rich unit of the Belluno Basin (Fig. 4, 16 m thick) correlates with an appreciable increase in  
53  
54 642 the sponge-spicule content, likely reflecting a more nutrient-rich mesotrophic environment. Such  
55  
56 643 mesotrophic conditions could have been related to an accelerated hydrological cycle linked to  
57  
58 644 introduction of isotopically light  $\text{CO}_2$  into the atmosphere and subsequent global warming. The  
59  
60

1  
2  
3 645 deleterious effects of nutrient excess on shallow-water carbonate production by reducing water  
4  
5 646 transparency, and encouraging bioeroding organisms is well documented (Hallock and Schlager, 1986,  
6  
7 647 Schlager, 2005). Consequently, the hiatus in the Verzegnis section between the chert-rich and  
8  
9 648 calcarenitic units in the upper part of the Soverzene Fm., supposedly representing the Late  
10  
11 649 Sinemurian–Early Pliensbachian interval, could in part be related to the postulated coeval drop in the  
12  
13 650 carbonate production on the neighbouring carbonate platforms. Since the lower portion of Soverzene  
14  
15 651 Fm. represents peri-platform oozes in which pelagic material, falling through the water column, has  
16  
17 652 been mixed with carbonate mud supplied by the adjacent platforms ('peri-platform ooze' of Schlager  
18  
19 653 and James, 1978), the drop of the carbonate precipitation and secretion in the shallow-water feeder  
20  
21 654 areas, acting together with the Sinemurian/Pliensbachian carbon-cycle boundary event recognized on  
22  
23 655 the Trento platform by Franceschi *et al.* (2014), could have produced the basinal starvation that caused  
24  
25 656 this hiatus.

26  
27  
28  
29 657 The onset of the calcarenitic unit at the top of the Monte Zugna Fm. in many localities represents a  
30  
31 658 fundamental reorganization of the palaeogeography during the interval of the major negative CIE: tidal  
32  
33 659 flat areas across much of the Tethyan area were replaced by subtidal, wave-controlled, oolitic shoals, in  
34  
35 660 which peritidal facies are missing. The only exception in the Southern Alps is the Adige Valley (Chizzola  
36  
37 661 section, Fig. 7) where Masetti *et al.* (1998) interpreted these remnants of the former peritidal system as  
38  
39 662 small tidal flats developed behind the western marginal shoals of the Trento Platform. The calcarenitic  
40  
41 663 unit at the top of the Monte Zugna Formation, like the overlying Loppio Oolitic Limestone, has been  
42  
43 664 interpreted as due to the retrogradation of the marginal carbonate sand bars located at the western  
44  
45 665 margin of the Trento Platform during a relative sea-level rise (Masetti *et al.*, 1998). At its most extreme,  
46  
47 666 this deepening and transgressive phase in the eastern Southern Alps coincided with the definitive  
48  
49 667 loss/drowning of Early–Late Sinemurian peritidal platforms, inherited from the Late Triassic, which  
50  
51 668 were located in many other areas around the Mediterranean (e.g. western Southern Alps, Ligurian  
52  
53 669 Alps, Northern Apennines, western and eastern Sicily, and High Atlas).  
54  
55  
56  
57  
58  
59  
60

1  
2  
3 670 Previous authors have postulated an interaction between tectonic and eustatic processes as the most  
4  
5 671 viable mechanism able to explain the transgressive phase that occurred at the boundary between the  
6  
7 672 Early and Late Sinemurian stages. Tectonic and/or eustatic processes were probably important, given  
8  
9 673 the significant rise in the *turneri* Zone of the putative eustatic sea-level curve of Haq *et al.* (1988) and the  
10  
11 674 north European relative sea-level curve of Hesselbo and Jenkyns (1998). However, taking in account  
12  
13 675 the coeval carbon-isotope excursion described herein, this relative sea-level rise in the Southern Alps  
14  
15  
16 676 and elsewhere in the Tethyan region could be interpreted not as purely eustatic but as the  
17  
18 677 consequence of a simultaneous decrease in carbonate production in shallow-water platforms caused  
19  
20 678 by introduction into the atmosphere-ocean system of isotopically light carbon that led to increased  
21  
22 679 introduction of terrestrially derived nutrients and ocean acidification, hence suppressing carbonate  
23  
24 680 production and deposition (cf., Trecalli *et al.*, 2012)..

25  
26  
27 681 This climatic event, acting together with a reactivation of the syn-sedimentary extensional tectonics that  
28  
29 682 reduced the productive areas of the carbonate platforms, would have ensured that the top of the  
30  
31 683 carbonate platforms could no longer be readily maintained at sea level. Such a proposed decrease in  
32  
33 684 carbonate production is also suggested by a fall in the sedimentation rate: the thickness of the  
34  
35 685 calcarenitic units, in both the Friuli and Trento Platforms is about 30 m (Foza and Monte Cumieli  
36  
37 686 sections) and a little thinner (about 20 m) in the Chizzola section, likely corresponding to the *turneri*,  
38  
39 687 *obtusum* and *oxynotum* Zones (~ 10m/Ma sedimentation rate). Assuming a thickness of about 100 m  
40  
41 688 for the lower peritidal unit of the Monte Zugna Formation (Masetti *et al.* 1998) and referring it to the  
42  
43 689 remaining part of the Early Sinemurian (*semicostatum* and *bucklandi* zones) and to the Hettangian, the  
44  
45 690 corresponding time span could be estimated as about 4 Ma according to the time scale of Gradstein *et*  
46  
47 691 *al.* (2012): that is, a sedimentation rate (~ 25 m/Ma) more than twice that of the calcarenitic unit.

48  
49  
50 692 The development of oolitic limestones in the run-up to the demise of the carbonate factory is a  
51  
52 693 widespread feature in many platforms of the Tethys (Trecalli *et al.* 2012 and references therein).

53  
54  
55 694 Recently, Trecalli *et al.* (2012) proposed for the early Toarcian oceanic anoxic event, recorded in the  
56  
57 695 Apennine carbonate platform, a model involving ocean water acidification, forced by CO<sub>2</sub> release at the

1  
2  
3 696 beginning of the event, followed by a calcification overshoot, driven by the recovery of ocean alkalinity.  
4  
5 697 According to this model, the negative CIE occurred over a short time interval during a biocalcification  
6  
7 698 crisis followed by a rebound of the  $\delta^{13}\text{C}$  curve towards more positive values corresponding to the  
8  
9 699 deposition of the oolitic units.

10  
11 700 Obvious evidence for the mesotrophic environments recorded by the chert-rich unit of the Verzegnis  
12  
13 701 section in the Belluno Basin is apparently missing in the palaeontological assemblage in the  
14  
15 702 shallow-water calcarenitic units at the top of the Monte Zugna Fm. On the contrary, the first appearance  
16  
17 703 of the *Paleomayncina termieri* and, more generally, an enrichment of foraminifera with a complex wall  
18  
19 704 structure, seem to be related to an amelioration of the environment and to a shift towards an  
20  
21 705 oligotrophic regime as proposed, for example, by Fugagnoli (2004) for the overlying Rotzo Fm. This  
22  
23 706 anomaly could be explained assuming that trophic conditions are not the main parameter controlling  
24  
25 707 the development of these foraminifera. Analysing in detail the behaviour of the carbonate factory with  
26  
27 708 respect to the isotopic excursions in all the three shallow-water sections suggests that the first negative  
28  
29 709 CIE, centred around the boundary of the *semicostatum* and *turneri* Zones (Fig. 8), coincides with the  
30  
31 710 stratigraphic level recording the loss of peritidal sediments; and their replacement by subtidal shoals  
32  
33 711 coincides with the interval of transition between negative and positive excursions of the isotopic curve.  
34  
35 712 These shoals are composed of ooids with a dense micritic ultrastructure (Fig. 6a), typically associated  
36  
37 713 with oncoids and dasycladaleans (*Palaeodasycladus mediterraneus*, *Palaeodasycladus gracilis*). The  
38  
39 714 recovery of the platform during the positive *turneri*-Zone CIE caused its progradation outwards and the  
40  
41 715 deposition of the fine-grained lagoonal *Gervillia buchi* beds on top of the marginal oolitic deposits of the  
42  
43 716 Chizzola and Foza sections, respectively at the western and eastern margin of the Trento Platform. In  
44  
45 717 the Friuli Platform (Cumieli section) the *Gervillia* beds are not recorded and are replaced by micritic  
46  
47 718 deposits lacking obvious macrofossils.

48  
49 719 The negative *obtusum*–*oxynotum* Zone excursion, which may be interpreted as due to a further  
50  
51 720 introduction of isotopically light carbon into the ocean–atmosphere system, can similarly be linked to a  
52  
53 721 reduction in carbonate production and a new transgression, recorded everywhere in the upper portion  
54  
55  
56  
57  
58  
59  
60

1  
2  
3 722 of calcarenitic unit of the Monte Zugna Fm. Being similar in bed organization and sedimentary  
4  
5 723 structures to the lower part of calcarenitic unit, this upper portion shows a vertical evolution in which  
6  
7 724 micritic ooids and dasycladaleans are replaced upward by radial-fibrous ooids and foraminifera with a  
8  
9 725 calcitic wall structure (Fig. 6b). The degree of water turbulence and velocity, as denoted by sedimentary  
10  
11 726 structures, apparently changed little during deposition of the unit, ruling out physical environmental  
12  
13 727 factors as controlling ooidal ultrastructure. Notably, the micritic ooids are associated with aragonitic  
14  
15 728 dasycladaleans and correlate with transitions between positive and negative excursions of the CIE,  
16  
17 729 whereas the radial-fibrous ooids are associated with foraminifera with calcitic walls during the acme of  
18  
19 730 the CIE. These associations point to seawater pH, in turn forced by CO<sub>2</sub> release, as a leading factor  
20  
21 731 controlling both fossil occurrence and ooidal structure by promoting short-term changes in the  
22  
23 732 dominant mineralogy (aragonite vs calcite) of the carbonate factory (e.g., Sandberg, 1983; Wilkinson  
24  
25 733 and Given, 1986; Zhuraviev and Wood, 2009). Following Strasser's (1986) study of Lower Cretaceous  
26  
27 734 limestones in France and Switzerland (1986), the micritic ooids are interpreted as originally aragonitic  
28  
29 735 which, after inversion to calcite, preserved some degree of original concentric structure, whereas the  
30  
31 736 radial-fibrous ooids, formed in waters of relatively low pH, preserved the original calcitic composition  
32  
33 737 and crystallographic orientation. Because a negative pulse of the carbon-isotope curve corresponds  
34  
35 738 with a transgressive trend of the sedimentary succession, and the positive excursion records the  
36  
37 739 contrary, the seawater pH may have directly controlled the whole production of the carbonate platform  
38  
39 740 and hence sedimentary accumulation rate and relative sea level.

40  
41 741 In the mid–Late Pliensbachian, the carbonate factory moved laterally from the top of the platform into  
42  
43 742 the neighbouring Belluno Basin, incorporating the portion of the basin corresponding to the Monte  
44  
45 743 Verzegnis area into a shallow-water domain where the cross-bedded calcarenitic unit at the top of the  
46  
47 744 Soverzene Fm. (interpreted as subtidal shoals) started to accumulate (Fig. 4; Zanferrari *et al.*, 2013).  
48  
49 745 During the same interval, a lack of accommodation space is assumed to have prevented deposition of  
50  
51 746 shallow-water deposits in the adjacent Friuli Platform (Monte Cumieli section; Zanferrari *et al.*, 2013).  
52  
53 747 The calcarenitic unit at the top of the Soverzene Fm. is in turn truncated by a hard-ground surface  
54  
55  
56  
57  
58  
59  
60

1  
2  
3 748 intervening between its upper boundary and the Verzegnis Encrinites. Since this latter unit  
4  
5 749 corresponds to the Early Bajocian to Early Callovian interval, the hard-ground surface is equivalent to  
6  
7 750 a time span extending from the Toarcian to the Aalenian, a hiatus equivalent to that separating the top  
8  
9  
10 751 of the Rotzo Fm. from the Lower Rosso Ammonitico in the central-western sector of the Trento  
11  
12 752 Platform (see above and Masetti *et al.* 1998).

13  
14 753 After the postulated Sinemurian event, the Pliensbachian recolonization seems to have been largely  
15  
16 754 controlled by an extensional tectonic phase that led to the first differentiation of the central-western and  
17  
18 755 northern-eastern sector of the Trento Platform in which accommodation space regulated the thickness  
19  
20 756 of the shallow-water succession. In the more subsident central-western sector of the Trento Platform,  
21  
22 757 the available accommodation space allowed the onset of a new type of carbonate factory  
23  
24 758 characterized, at the beginning, by eutrophic deposits with abundant marls and lenses of black shales,  
25  
26 759 followed by the development of the “*Lithiotis*” beds (Rotzo Fm.; Masetti *et al.* 1998; Bassi *et al.* 1999;  
27  
28 760 Posenato and Masetti 2012). This Early Pliensbachian environmental deterioration could be also  
29  
30 761 ascribed to the climatic events that occurred at the Sinemurian/Pliensbachian boundary (Hesselbo and  
31  
32 762 Korte, 2012; Franceschi *et al.* 2014) or, more likely, to the cumulative effects of both the preceding  
33  
34 763 “*Arnioceras* time” and the S/P boundary events. According to Posenato & Masetti (2012), it is likely that  
35  
36 764 the Rotzo Fm., overlying the Monte Zugna Fm., is separated by a depositional hiatus referable to part  
37  
38 765 of the Early Pliensbachian. Other evidence of mesotrophic conditions during “*Arnioceras* time” comes  
39  
40 766 from the Umbro–Marchean Apennines where peritidal deposits of the Calcare Massiccio pass upward  
41  
42 767 into a deeper water succession characterized by the prevalence of sponges and other filter-feeding  
43  
44 768 organisms (“Calcare Massiccio B”, from *semicostatum* (Lower Sinemurian) to *jamesoni* Zones (Lower  
45  
46 769 Pliensbachian) following Marino and Santantonio (2010).

50  
51  
52  
53 770 In the north-eastern portion of the Trento Platform and in the northern edge of the Friuli Platform, where  
54  
55 771 no accommodation space was available, the top of the Monte Zugna Fm. is truncated by an  
56  
57 772 unconformity surface corresponding to the gap embracing the Pliensbachian, Toarcian and Aalenian  
58  
59  
60

1  
2  
3 773 stages (about 20 Ma, Gradstein *et al.* 2012), sporadically interrupted by the emplacement of the  
4  
5 774 crinoidal sand waves of the Fanes Piccola Encrinite (Masetti *et al.* 1998, Zanferrari *et al.*, 2013). The  
6  
7 775 lithostratigraphic relationships depicted in Figure 3 suggest that this huge hiatus could be related to the  
8  
9 776 interplay between negligible accommodation space, with the top of the Trento Platform fixed at sea-level  
10  
11 777 for more than 20 Ma, and the deleterious effects on the carbonate factory of at least four climatic  
12  
13 778 events: that of the “*Arnioceras* time” described here, the Sinemurian/Pliensbachian boundary event,  
14  
15 779 the mid–Pliensbachian warming event and the Toarcian OAE.

## 18 19 780 **6.0 SUMMARY AND CONCLUSIONS**

20  
21 781 Starting from the documented demise and/or drowning of several Tethyan carbonate platforms at some  
22  
23 782 point during the Sinemurian Stage, a chemostratigraphic transect through this interval has been  
24  
25 783 performed across the whole domain of the Eastern Southern Alps to investigate the response of both  
26  
27 784 shallow- and deep-water domains during this time interval. Investigation has concentrated on  
28  
29 785 carbonate-platform successions, locally underlying open-marine and/or pelagic cover, and one basinal  
30  
31 786 peri-platform succession. An abrupt positive followed by a broader negative carbon-isotope excursion,  
32  
33 787 typically in the range of 0.5–1.0 ‰, has been detected in all 4 stratigraphic sections over the likely  
34  
35 788 stratigraphical extent of the ammonite *Arnioceras* that is recorded from the deep-water basinal  
36  
37 789 succession. The positive excursion is attributed to the *turneri* Zone and the following negative  
38  
39 790 excursion likely centred in the *obtusum* Zone (Figs 5, 8).

40  
41 791 In the Belluno Basin, filled by peri-platform oozes (Monte Verzegnis section: deep-water Soverzene  
42  
43 792 Fm.), the negative CIE spans a stratigraphic thickness of about 60 m and its lowest value is located  
44  
45 793 immediately below the base of a chert-rich unit corresponding to an increase in the sponge content of  
46  
47 794 the sediment. The hiatus between the chert-rich and calcarenitic units in the upper part of the  
48  
49 795 Soverzene Fm. is considered to embrace the Late Sinemurian–Early Pliensbachian, an interval  
50  
51 796 missing in both the shallow-water Monte Cumieli and Foza sections, and could be related to the coeval  
52  
53 797 postulated drop in the sediment production of the feeder carbonate platforms.  
54  
55  
56  
57  
58  
59  
60

1  
2  
3 798 In the shallow-water carbonate succession of the Monte Zugna Formation (Monte Cumieli, Foza,  
4  
5 799 Chizzola sections), the correlative major carbon-isotope negative excursion is mainly developed within  
6  
7 800 the calcarenitic unit at its top, which is divided into two parts (*semicostatum*–*turneri* Zones and  
8  
9 801 *obtusum* Zone, respectively, for the lower and upper parts) by the lagoonal *Gervillia buchi* beds,  
10  
11 802 indicating an apparent rapid recovery of the platform (*turneri* Zone, Figs 4, 7 and 8). The different  
12  
13 803 ooidal structures and fossil assemblages characterizing the two calcarenitic units (Fig. 6) could have  
14  
15 804 been a result of changes in pH that, operating on a scale of few thousands of years, favoured first  
16  
17 805 ‘aragonitic’ and then ‘calcite seas’. The virtual lack of fine-grained carbonate in the succession during  
18  
19 806 the negative excursion may thus be explained if the switch to calcite seas also controlled the  
20  
21 807 production of aragonitic mud, whether inorganically precipitated or derived from biological sources.  
22  
23 808 These considerations, coupled with a fall in sedimentation rate to half the value of the preceding  
24  
25 809 peritidal platforms, suggests that the transgression recorded by the calcarenitic unit that came to  
26  
27 810 overlie the lower peritidal unit of the Monte Zugna Fm. and well documented by sea-level curves  
28  
29 811 reconstructed for the Early/Late Sinemurian interval, could be the consequence, not of a purely  
30  
31 812 eustatic oscillation, but also a decrease in carbonate production. The lateral spread of this calcarenitic  
32  
33 813 unit represents a potential first step towards the demise and ultimate drowning of the  
34  
35 814 platforms.  
36  
37 815 The re-colonization of the Trento Platform after the “Arnioceras time” climatic event was controlled by  
38  
39 816 extensional tectonics governing the availability of accommodation space: where such space was  
40  
41 817 negligible, the top of the Monte Zugna Fm. is truncated by a huge unconformity surface corresponding  
42  
43 818 to a hiatus spanning the Late Sinemurian to the Early Bajocian (about 20 Ma); in the more subsident  
44  
45 819 central-western sector, the available accommodation space allowed the onset of a new type of subtidal  
46  
47 820 carbonate factory characterized by the Pliensbachian “Lithiotis facies”.  
48  
49  
50  
51  
52  
53  
54  
55 821 The negative  $\delta^{13}\text{C}$  excursion may be attributed to a reduction of global biomass and/or burial of  
56  
57 822 organic matter and/or introduction of  $^{13}\text{C}$ -depleted  $\text{CO}_2$  into the atmosphere–ocean system from a  
58  
59  
60



1  
2  
3 823 buried source of isotopically light carbon. A coeval negative excursion in  $\delta^{13}\text{C}$ , described from  
4  
5 824 southern England, is accompanied by palynological evidence suggesting the onset of a major  
6  
7 825 warming event. The data presented here demonstrate that the major negative CIE of “Arnioceras time”  
8  
9  
10 826 is represented across the entire eastern Southern Alps, invariably associated with environmental  
11  
12 827 reorganization of carbonate platforms and regional deepening. Taking in account also the widespread  
13  
14 828 occurrence of definitive demise and drowning during the Sinemurian Stage in many parts of the  
15  
16 829 Tethyan area, the negative CIE likely represents a global climatic event that pre-conditioned many  
17  
18 830 carbonate platforms for demise and drowning.  
19

## 20 21 831 **7.0 Acknowledgements**

22  
23  
24 832 We are grateful to: Federico Venturi (Perugia University), who determined the *Arnioceras* specimen  
25  
26 833 in the field; Giulio Pavia (Turin University) helped us in recognizing other ammonite specimens coming  
27  
28 834 from condensed units in the Verzegnis section; Elisabetta Erba examined basinal samples for  
29  
30 835 nannoplankton; Marco Avanzini (MuSe, Trento) supplied the logistic help that made possible the  
31  
32 836 sampling of the Chizzola section; Guido Roghi, Jacopo del Corso (Padua University) and Marco  
33  
34 837 Franceschi (MuSe, Trento) lent a hand in the field during the chemostratigraphic sampling of the same  
35  
36 838 section. Isotopic analyses in Oxford were facilitated by Norman Charnley, Chris Day and Alan Hsieh.  
37  
38  
39 839 Karl Föllmi reviewed the manuscript. This research was supported by project PRIN 2008: Demise of  
40  
41 840 the carbonate platforms in the Sinemurian - Pliensbachian time: a new global event? - National  
42  
43 841 coordinator: Daniele Masetti.  
44  
45

## 46 47 842 **References**

48  
49  
50 843 AVANZINI, M., FRISIA, S., KEPPENS, E. & VAN DEN DRIESSCHE, K., 1997. A dinosaur tracksite in an Early  
51  
52 844 Jurassic tidal flat in Northern Italy: palaeoenvironmental reconstruction from sedimentology and  
53  
54 845 geochemistry. *Palaios* **12**, 538–551.  
55  
56  
57  
58  
59  
60

- 1  
2  
3 846 BECCARELLI-BAUCK, L., 1988. Unter-bismitteljurassische Karbonatformationen am Westrand der  
4  
5 847 Trento-Plattform (Südalpen, Norditalien). *Münchener Geowissenschaftliche Abhandlung* **13**, 1–86.  
6  
7  
8 848 BARATTOLO F. & ROMANO R., 2005. Shallow carbonate platform bioevents during the Upper Triassic–  
9  
10 849 Lower Jurassic: an evolutive interpretation. *Bollettino della Società Geologica Italiana* **124**, 123–142.  
11  
12  
13 850 BASSI, D., BOOMER, I., FUGAGNOLI, A., LORIGA, C., POSENATO R. & WHATLEY, R. C., 1999. Faunal  
14  
15 851 assemblages and palaeoenvironment of shallow water black shales in the Tonezza area (Calcarei Grigi,  
16  
17 852 Early Jurassic, Southern Alps). *Annali dell'Università degli Studi di Ferrara, Sezione di Scienze della*  
18  
19 853 *Terra* **8**, 1–16.  
20  
21  
22  
23 854 BELLANCA, A., MASETTI, D., NERI, R. & VENEZIA, F., 1999. Geochemical and sedimentological evidence of  
24  
25 855 productivity cycles recorded in Toarcian black shales from the Belluno Basin, Southern Alps, northern  
26  
27 856 Italy. *Journal of Sedimentary Research* **69**, 466–476.  
28  
29  
30  
31 857 BERNOULLI, D. & JENKYN, H. C., 1974. Alpine, Mediterranean and central Atlantic Mesozoic facies in  
32  
33 858 relation to the early evolution of the Tethys. In *Modern and Ancient Geosynclinal Sedimentation*, Edited  
34  
35 859 by R. H. Dott, Jr and R. H. Shaver, *SEPM Special Publication* **19**, 129–160.  
36  
37  
38  
39 860 BERTOTTI, G., PICOTTI, V., BERNOULLI, D. & CASTELLARIN, A., 1993. From rifting to drifting: tectonic  
40  
41 861 evolution of the South-Alpine upper crust from the Triassic to the Early Cretaceous. *Sedimentary*  
42  
43 862 *Geology* **86**, 53–76.  
44  
45  
46 863 BILL, M., O' DOHERTY L., GUÉX J., BAUMGARTNER P. O. & MASSON H., 2001. Radiolarite ages in Alpine–  
47  
48 864 Mediterranean ophiolites: constraints on the oceanic spreading and the Tethys–Atlantic connection.  
49  
50 865 *Geological Society of America Bulletin* **113**, 129–143.  
51  
52  
53  
54 866 BOSELLINI, A. & BROGLIO LORIGA, C., 1971. I “Calcarei Grigi” di Rotzo (Giurassico inferiore, Altopiano di  
55  
56 867 Asiago) e loro inquadramento nella paleo-geografia e nella evoluzione tettonico-sedimentaria delle  
57  
58  
59  
60

- 1  
2  
3 868 Prealpi venete. *Annali dell'Università di Ferrara (Sezione Scienze Geologiche e Paleontologiche)* **5**, 1–  
4  
5 869 61.  
6  
7 870 BOSELLINI, A. & MASETTI, D., 1972. Ambiente e dinamica deposizionale del Calcare del Vajont  
8  
9 871 (Giurassico medio, Prealpi Bellunesi e Friulane. *Annali dell'Università di Ferrara (Sezione Scienze*  
10  
11 872 *Geologiche e Paleontologiche)* **5**, 87–100.  
12  
13 873 BOSELLINI, A., MASETTI, D. & SARTI, M., 1981. A jurassic "Tongue of the Ocean" infilled with oolitic sands:  
14  
15 874 the Belluno Trough, venetian Alps, Italy. *Marine Geology* **44**, 55–95.  
16  
17  
18 875 CHIOCCHINI M., FARINACCI A., MANCINELLI A., MOLINARI V. & POTETTI M., 1994, Biostratigrafia a  
19  
20 876 foraminiferi, dasycladali e calpionelle delle successioni carbonatiche mesozoiche dell'Appennino  
21  
22 877 centrale (Italia). *Studi Geologici Camerti*, Camerino, volume speciale "Biostratigrafia dell'Italia centrale"  
23  
24 878 p. 9–128.  
25  
26  
27 879 CHIOCCHINI, M., CHIOCCHINI, R. A., DIDASKALOU, P. & POTETTI, M. (2008): Ricerche micropaleontologiche  
28  
29 880 e biostratigrafiche sul Mesozoico della piattaforma carbonatica laziale-abruzzese (Italia centrale).  
30  
31 881 *Memorie descrittive Carta Geologica Italiana* **84**, 5–170.  
32  
33  
34 882 CLAPS M., ERBA, E., MASETTI D. & MELCHIORRI F., 1995 - Milankovitch-type cycles recorded in Toarcian  
35  
36 883 black-shales from the Belluno Trough (Southern Alps, Italy). *Memorie Scienze Geologiche Padova* **47**,  
37  
38 884 179–188  
39  
40  
41 885 COBIANCHI, M., 2002. I nannofossili calcarei del Giurassico medio e superiore del Bacino di Belluno  
42  
43 886 (Alpi Meridionali). *Atti Ticinensi di Scienze della Terra* **43**, 3–24.  
44  
45  
46 887 CUVILLIER, J., FOURY, G. & PIGNATTI MORANO, A., 1968. Foraminiferes nouveaux du Jurassique superieur  
47  
48 888 du Val Cellina (Frioul Occidental, Italie). *Geologica Romana* **7**, 141–155.  
49  
50  
51 889 COURTILOT, V.E. & RENNE, P.R., 2003. On the ages of flood basalt events. Sur l'ages des trappes  
52  
53 890 basaltiques. *C.R. Geosciences* **335**, 113–140.  
54  
55  
56 891 D'ARGENIO, B., PESCATORE, T. & SCANDONE, P., 1973. *Schema geologico dell'Appennino meridionale*  
57  
58 892 *(Campania e Lucania)*. *Quaderni Accademia Nazionale dei Lincei, Convegno sul tema: Moderne*  
59  
60 893 *vedute sulla geologia dell'Appennino* **183**, 49–82.

- 1  
2  
3 894 DAVEY, S. D. & JENKYN, H. C., 1999. Carbon-isotope stratigraphy of shallow-water limestones and  
4  
5 895 implications for the timing of Late Cretaceous sea-level rise and anoxic events (Cenomanian-Turonian  
6  
7 896 of the peri-Adriatic carbonate platform, Croatia). *Eclogae Geologicae Helvetiae* **92**, 163–170.  
8  
9  
10 897 DE CARLIS, A. & LUALDI, A., 2010. Synrift sedimentation on the northern Tethys margin: an example from  
11  
12 898 the Ligurian Alps (Upper Triassic to Lower Cretaceous, Prepiemont domain, Italy). *International*  
13  
14 899 *Journal of Earth Sciences* **100**, 1589–1604.  
15  
16 900 DE CASTRO P., 1991. Jurassic. In: *5th International Symposium on Fossil Algae. Capri. 7–12 april 1991.*  
17  
18 901 *Field-Trip Guide book.*  
19  
20  
21 902 DOMMERGUES, J. L., FERRETTI, A. & MEISTER, C., 1994. Les faunes d'ammonites du Sinémurien de  
22  
23 903 l'Apennin Central (Marches et Toscane, Italie). *Bollettino della Società Paleontologica Italiana* **33(1)**,  
24  
25 904 13–42.  
26  
27  
28 905 FANTONI, R. & SCOTTI, P., 2003. Thermal record of the Mesozoic extensional tectonics in the Southern  
29  
30 906 Alps: *Atti Ticinensi Scienze della Terra* **9**, 96–101..  
31  
32 907 FÖLLMI, K. B., WEISSERT, H., BISPING, M. & FUNK, H., 1994. Phosphogenesis, carbon-isotope  
33  
34 908 stratigraphy, and carbonate-platform evolution along the Lower Cretaceous northern Tethyan margin.  
35  
36 909 *Geological Society of American Bulletin* **106**, 729–746.  
37  
38  
39 910 FRANCESCHI, M., DAL CORSO, J., POSENATO, R., ROGGI, G., MASETTI, D. & JENKYN, H. C., 2014. Early  
40  
41 911 Pliensbachian (Early Jurassic) C-isotope perturbation and the diffusion of the *Lithiotis* Fauna: Insights  
42  
43 912 from the western Tethys. *Palaeogeography, Palaeoclimatology, Palaeoecology* **410**, 255–263.  
44  
45 913 FUGAGNOLI, A. (2004). Trophic regimes of benthic foraminiferal assemblages in Lower Jurassic  
46  
47 914 shallow water carbonates from northeastern Italy (Calcarei Grigi, Trento Platform, Venetian Prealps).  
48  
49 915 *Palaeogeography, Palaeoclimatology, Palaeoecology* **205 (1–2)**, 111–130.  
50  
51  
52 916 GAETANI, M., 1975. Jurassic stratigraphy of the Southern Alps: a review. In C. Squyres, ed.,  
53  
54 917 *Geology of Italy; Libyan Arab Republic Earth Sci. Soc* 377–402.  
55  
56 918 Gradstein, F. M, Ogg, J. G. & Schmitz, M. D. Eds, 2012. *The Geologic Time Scale, 2012.*  
57  
58  
59  
60

- 1  
2  
3 919 Boston, USA, Elsevier.
- 4  
5 920 GRÖTSCH, J., BILLING, I. & VAHRENKAMP, V.C., 1998. Carbon isotope stratigraphy in shallow-water  
6  
7 921 carbonates: implications for Cretaceous black-shale deposition. *Sedimentology* **45**, 623–634.
- 8  
9 922 HAQ, B. U., HARDENBOL, J. & VAIL, P. R., 1988. Mesozoic and Cenozoic chronostratigraphy and  
10  
11 923 cycles of sea-level change. In: Wilgus, C. K., Hastings, B. S. & Kendall, C. G. St. C.,  
12  
13 924 Posamentier, H. W., Ross C.A. Van Wagoner, J. C. (eds.), *Sea-Level Changes: An Integrated*  
14  
15 925 *Approach. SEPM Special Publication* **42**, 71–108.
- 16  
17  
18 926 HALLOCK, P. & SCHLAGER, W., 1986. Nutrient excess and the demise of coral reefs and carbonate  
19  
20 927 platforms. *Palaios* **1**, 389–398.
- 21  
22  
23 928 HERMOSO, M., MINOLETTI, F., RICKABY, R. E. M., HESSELBO, S. P., BAUDIN, F. & JENKYNS, H. C.,  
24  
25 929 2012. Dynamics of a stepped carbon-isotope excursion: ultra high-resolution study of Early  
26  
27 930 Toarcian environmental change. *Earth and Planetary Science Letters* **319–320**, 45–54.
- 28  
29  
30 931 HESSELBO, S. P. & JENKYNS, H. C., 1998. Sequence stratigraphy of the Lower Jurassic of the  
31  
32 932 British Isles. In: de Graciansky, P. C., Hardenbol, J., Jaquin, T., Vail, P. R. & Farley, M.B. (Eds),  
33  
34 933 *Mesozoic and Cenozoic Sequence Stratigraphy of Europe, Special Publication of the Society of*  
35  
36 934 *Economic Paleontologists and Mineralogists* **60**, 561–581.
- 37  
38  
39 935 HESSELBO, S. P., JENKYNS, H. C., DUARTE, L. V. & OLIVEIRA, L. C. V., 2007. Carbon-isotope record of the  
40  
41 936 Early Jurassic (Toarcian) Oceanic Anoxic Event from fossil wood and marine carbonate (Lusitanian  
42  
43 937 Basin, Portugal). *Earth and Planetary Science Letters* **253**, 455–470.
- 44  
45  
46 938 HUDSON, J. D., 1977. Stable isotopes and limestone lithification. *J. Geol. Soc. London*, **133**, 637–660.
- 47  
48 939 JENKYNS, H. C. 1971. Speculations on the genesis of crinoidal limestones in the Tethyan Jurassic.  
49  
50 940 *Geologische Rundschau* **60**, 471–488.
- 51  
52  
53 941 JENKYNS, H. C., 1988. The early Toarcian (Jurassic) anoxic event: stratigraphic, sedimentary, and  
54  
55 942 geochemical evidence. *American Journal of Sciences* **288**, 101–151.
- 56  
57  
58  
59  
60

- 1  
2  
3 943 JENKYNS, H. C., 2003. Evidence for rapid climate change in the Mesozoic–Palaeogene greenhouse  
4  
5 944 world. *Philosophical Transactions of the Royal Society of London, Series A* **361**, 1885–1916.  
6  
7 945 JENKYNS, H. C. & TORRENS H. S., 1971. Palaeogeographic evolution of Jurassic seamounts in Western  
8  
9 946 Sicily. In: Colloque du Jurassique méditerranéen, Edited by E. Végh-Neubrandt, *Annales Instituti*  
10  
11 947 *Geologici Publici Hungarici* **54/2**, 91–104.  
12  
13 948 JENKYNS, H. C., SARTI, M., MASETTI, D. & HOWARTH, M. K. 1985. Ammonites and stratigraphy of Lower  
14  
15 949 Jurassic black shales and pelagic limestones from the Belluno Trough, Southern Alps, Italy. *Eclogae*  
16  
17 950 *Geologicae Helveticae* **78**, 299–311.  
18  
19 951 JENKYNS, H. C., JONES, C. E., GRÖCKE, D. R., HESSELBO, S. P. & PARKINSON, D. N., 2002.  
20  
21 952 Chemostratigraphy of the Jurassic System: applications, limitations and implications for  
22  
23 953 palaeoceanography. *Journal of the Geological Society* **159**, 351–378.  
24  
25 954 JENKYNS, H.C. & WEEDON, G.P., 2013. Chemostratigraphy (CaCO<sub>3</sub>, TOC, δ<sup>13</sup>C<sub>org</sub>) of Sinemurian  
26  
27 955 (Lower Jurassic) black shales from the Wessex Basin, Dorset and palaeoenvironmental implications.  
28  
29 956 *Newsletters on Stratigraphy* **46**, 1–21.  
30  
31 957 JONES, C. E., JENKYNS, H. C. & HESSELBO, S. P., 1994. Strontium isotopes in Early Jurassic seawater.  
32  
33 958 *Geochimica Cosmochimica Acta* **58**, 1285–1301.  
34  
35 959 KEMP, D. B., COE, A. L., COHEN, A. S. & SCHWARK, L., 2005. Astronomical pacing of methane release in  
36  
37 960 the Early Jurassic period. *Nature* **437**, 396–399.  
38  
39 961 KORTE, C. & HESSELBO, S.P., 2011. Shallow marine carbon and oxygen isotope and elemental records  
40  
41 962 indicate icehouse-greenhouse cycles during Early Jurassic. *Paleoceanography* **26**, PA4219, doi:  
42  
43 963 10.1029/2011PA002160.  
44  
45 964 MARINO, M. & SANTANTONIO, M. (2010). Understanding the geological record of carbonate platform  
46  
47 965 drowning across rifted Tethyan margins: examples from the Lower Jurassic of the Apennines and  
48  
49 966 Sicily (Italy). *Sedimentary Geology* **225**, 116–137.  
50  
51 967 MARSHALL, J. D., 1992. Climatic and oceanographic isotopic signals from the carbonate rock record  
52  
53 968 and their preservation. *Geological Magazine* **129**, 143–160.  
54  
55  
56  
57  
58  
59  
60

- 1  
2  
3 969 MARTIRE, L. (2007). Rosso Ammonitico Veronese. In: Cita, M. B., Abbate, E., Balini, M., Conti, M. A.,  
4  
5 970 Falorni, P., Germani, D., Groppelli, G., Manetti, P. & Petti, F. M. (eds.), Carta Geologica d'Italia  
6  
7 971 1:50.000. Catalogo delle Formazioni, Unità tradizionali (1). APAT, Dipartimento Difesa del Suolo,  
8  
9 972 Servizio Geologico d'Italia, Quaderni del Servizio Geologico d'Italia **Serie III, 7 (VI)**, 98-100.  
10  
11 973 MARZOLI, A., RENNE, P. R., PICCIRILLO, E. M., ERNESTO, M., BELLINI, G. & DE MIN, A., 1999. Extensive  
12  
13 974 200-million-year-old continental flood basalts of the Central Atlantic Magmatic Province. *Science* **284**,  
14  
15 975 616–618.  
16  
17  
18 976 MASETTI D. & BOTTONI, A., 1975. L'Encrinite di Fanes e suo inquadramento nella paleogeografia  
19  
20 977 giurassica delle Dolomiti centro-occidentali. *Rivista Italiana di Paleontologia e Stratigrafia* **84**,  
21  
22 978 169-186.  
23  
24  
25 979 MASETTI, D. & BIANCHIN, G., 1987. Geologia del Gruppo dello Schiara (Dolomiti Bellunesi): suo  
26  
27 980 inquadramento nell'evoluzione giurassica del margine orientale della piattaforma di Trento. *Memorie*  
28  
29 981 *di Scienze Geologiche Padova* **39**, 187–212.  
30  
31 982 MASETTI, D., CLAPS, M., GIACOMETTI, A., LODI, P. & PIGNATTI, P., 1998. I Calcari Grigi della Piattaforma  
32  
33 983 di Trento (Lias inferiore e medio, Prealpi Venete). *Atti Ticinensi di Scienze della Terra* **40**, 139-183.  
34  
35  
36 984 MASETTI, D., FANTONI, R., ROMANO, R., SARTORIO, D. & TREVISANI, E., 2012. Tectonostratigraphic  
37  
38 985 evolution of the Jurassic extensional basins of the eastern Southern Alps and Adriatic foreland based  
39  
40 986 on an integrated study of surface and subsurface data. *American Association of Petroleum Geologists*  
41  
42 987 *Bulletin* **96**, 2065–2089.  
43  
44  
45 988 MASSARI F., 1981. Cryptalgal fabrics in the Rosso Ammonitico sequences in the Venetian Alps. In:  
46  
47 989 Farinacci, A. and Elmi, S., Eds., *Rosso Ammonitico Symposium Proceedings*, Edizioni Tecnoscienza,  
48  
49 990 Rome, 453–469.  
50  
51 991 MERINO-TOMÉ, O., DELLA PORTA, G., KENTER, J. A. M., VERWERK, K., HARRIS, P. M., ADAMS, E. W.,  
52  
53 992 PLAYTON, T. & CORROCHANO, D., 2012. Sequence development in an isolated carbonate platform  
54  
55 993 (Lower Jurassic, Djebel Bou Dahar, High Atlas, Morocco): influence of tectonics, eustacy and  
56  
57 994 carbonate production. *Sedimentology* **59**, 118–155.  
58  
59  
60

- 1  
2  
3 995 MEISTER, C., SCHIROLI, P., DOMMERGUES, J. L., 2009. Sinemurian to lowermost Toarcian ammonites of  
4  
5 996 the Brescian Prealps (Southern Alps, Italy): preliminary biostratigraphical framework and correlations.  
6  
7 997 *Volumina Jurassica* **7**, 9–18.
- 8  
9  
10 998 PAGE A., 2010. Stratigraphic framework. In: Lord, R. & Davis, P.G. (Eds), *Fossils from the Lower Lias*  
11  
12 999 *of the Dorset Coast, Palaeontological Association Field Guides to Fossils* **13**, 33–53.
- 13  
14 1000 PIANO, C. & CARULLI, G. B. 2002. Sedimentazione e tettonica giurassica nella successione del gruppo  
15  
16 1001 del Monte Verzegnis (Prealpi Carniche nord-orientali). In: Carulli, G. B. & Ponton, M. (eds), Atti  
17  
18 1002 dell'80<sup>a</sup> Riunione Estiva della Società Geologica Italiana, *Memorie della Società Geologica Italiana* **57**,  
19  
20 1003 115–122.
- 21  
22  
23 1004 PORTER, S. J., SMITH, P., CARUTHERS, A., HOUA, P., GRÖCKEB, D. R. & SELBYB, D., 2014. New high  
24  
25 1005 resolution geochemistry of Lower Jurassic marine sections in western North America: A global positive  
26  
27 1006 carbon isotope excursion in the Sinemurian. *Earth and Planetary Science Letters* **397**, 19–31.
- 28  
29  
30 1007 POSENATO, R. & MASETTI, D., 2012. Environmental control and dynamics of Lower Jurassic bivalve  
31  
32 1008 build-ups in the Trento Platform (Southern Alps, Italy). *Palaeogeography, Palaeoclimatology,*  
33  
34 1009 *Palaeoecology* **361–362**, 1–13.
- 35  
36 1010 RIDING, J. B., LENG, M. J., KENDER, S., HESSELBO, S. P. & FEIST-BURKHARDT, S., 2012. Isotopic and  
37  
38 1011 palynological evidence for a new Early Jurassic environmental perturbation. *Palaeogeography,*  
39  
40 1012 *Palaeoclimatology, Palaeoecology* **374**, 16–27.
- 41  
42  
43 1013 RONCHI, P., LOTTAROLI, F. & RICCHIUTO, T., 2000. Sedimentary and diagenetic aspects of the Liassic  
44  
45 1014 Inici Fm. and its stratigraphic context (Sicily Channel, Italy). *Memorie della Società Geologica Italiana,*  
46  
47 1015 **55**, 261–269.
- 48  
49  
50 1016 ROMANO, R., BARATTOLO, F. & MASETTI D., 2005. Biostratigraphic evidence of the middle Liassic hiatus  
51  
52 1017 in the Foza Section. (Eastern sector of the Trento Platform, Calcarei Grigi Formation, Venetian  
53  
54 1018 Prealps). *Bollettino della Società Geologica Italiana* **124**, 301–312.
- 55  
56 1019 RUIZ-ORTIZ, P. A., BOSENCE, D. W. J., REY, J., NIETO CASTRO, J. M., & MOLINA J.M., 2004. Tectonic  
57  
58 1020 control of facies architecture, sequence stratigraphy and drowning of a Liassic carbonate platform  
59  
60



- 1  
2  
3 1021 (Betic Cordillera, Southern Spain). *Basin Research* **16**, 235–257.
- 4  
5 1022 SABATINO, N., NERI, R., BELLANCA, A., JENKYN, H. C., BAUDIN, F., PARISI G. & MASETTI, D., 2009.
- 6  
7 1023 Carbon-isotope records of the Early Jurassic (Toarcian) oceanic anoxic event from the Valdorbia
- 8  
9 1024 (Umbria–Marche Apennines) and Monte Mangart (Julian Alps) sections: palaeoceanographic and
- 10  
11 1025 stratigraphic implications. *Sedimentology* **56**, 1307–1328.
- 12  
13  
14 1026 SABATINO, N., VLAHOVIĆ, I., JENKYN, H. C., SCOPELLITI, G., NERI, R., PRTOĀAN, B. & VELIĆ, I., 2013.
- 15  
16 1027 Carbon-isotope record and palaeoenvironmental changes during the early Toarcian anoxic event in
- 17  
18 1028 shallow-marine carbonates of the Adriatic Carbonate Platform in Croatia. *Geological Magazine* **150**,
- 19  
20 1029 1085–1102.
- 21  
22  
23 1030 SANDBERG, P. A., 1983. An oscillating trend in Phanerozoic non-skeletal carbonate
- 24  
25 1031 mineralogy. *Nature* **305**, 19–22.
- 26  
27 1032 SCHIROLLI, P., 1997. La successione liassica nelle Prealpi Bresciane, Centro-Occidentali (Alpi
- 28  
29 1033 Meridionali, Italia): stratigrafia, evoluzione paleogeografico-strutturale ed eventi connessi al rifting. *Atti*
- 30  
31 1034 *Ticinensi di Scienze della Terra* **6**, 5–137.
- 32  
33  
34 1035 SCHLAGER, W., 2005 Carbonate Sedimentology and Sequence Stratigraphy. *SEPM Concepts in*
- 35  
36 1036 *Sedimentology and Paleontology* No. 8, 1–198.
- 37  
38 1037 SCHLAGER, W. & JAMES N. P. 1978. Low-Magnesium calcite limestone forming at the deep-sea floor,
- 39  
40 1038 tongue of the Ocean, Bahamas. *Sedimentology* **25**, 675–702.
- 41  
42  
43 1039 SCHOLLE, P. & ARTHUR, M. A. 1980. Carbon isotope fluctuations in Cretaceous pelagic limestones:
- 44  
45 1040 potential stratigraphic and petroleum exploration tool. *American Association of Petroleum Geologists*
- 46  
47 1041 *Bulletin* **64**, 67–87.
- 48  
49 1042 SEPTFONTAINE M., 1984. Biozonation (à l'aide des Foraminifères imperforés) de la plate-forme interne
- 50  
51 1043 carbonatée liassique du Haut Atlas (Maroc). *Revue de Micropaléontologie* **27**, 209–229.
- 52  
53  
54 1044 SEPTFONTAINE M., 1985. Milieux de dépôts et Foraminifères (Lituolidés) de la plate-forme carbonatée
- 55  
56 1045 du Lias moyen au Maroc. *Revue de Micropaléontologie* **28**, 265–289.
- 57  
58 1046 STRASSER, A., 1986. Ooids in Purbeck limestones (lowermost Cretaceous) of the Swiss and French
- 59  
60

- 1  
2  
3 1047 Jura. *Sedimentology* **33**, 711–728.  
4  
5 1048 SWART, P.K., 2008, Global synchronous changes in the carbon isotopic composition of carbonate  
6  
7 1049 sediments unrelated to changes in the global carbon cycle. *Proceeding of the National Academy of*  
8  
9 1050 *Sciences* **105**, 13741–13745.  
10  
11 1051 TRECALI, A., SPANGENBERG, J., ADATTE, T., FOLLM, K. B. & PARENTE, M., 2012. Carbonate platform  
12  
13 1052 evidence of ocean acidification at the onset of the early Toarcian oceanic anoxic event. *Earth and*  
14  
15 1053 *Planetary Science Letters* **357–358**, 214–225.  
16  
17 1054 WENDT, J. 1969. Die stratigraphisch-paläogeographische Entwicklung des Jura in Westsizilien.  
18  
19 1055 *Geologische Rundschau* **58**, 735–755.  
20  
21 1056 WILKINSON, B.H. & GIVEN, R.K., 1986. Secular variation in abiotic marine carbonates: constraints on  
22  
23 1057 Phanerozoic atmospheric carbon dioxide contents and oceanic Mg/Ca ratios. *Journal of Geology* **94**,  
24  
25 1058 321–333.  
26  
27 1059 WILMSEN, M. & NEUWEILER, F., 2008. Biosedimentology of the Early Jurassic post-extinction carbonate  
28  
29 1060 depositional system, central High Atlas rift basin, Morocco. *Sedimentology* **55**, 773–807.  
30  
31 1061 WINTERER, E. L. & BOSELLINI, A., 1981. Subsidence and Sedimentation on Jurassic Passive  
32  
33 1062 Continental Margin, Southern Alps, Italy. *American Association of Petroleum Geologists Bulletin* **65**,  
34  
35 1063 394–421.  
36  
37 1064 WOODFINE, R. G., JENKYN, H. C., SARTI, M., BARONCINI, F. & VIOLANTE C., 2008. The response of two  
38  
39 1065 Tethyan carbonate platforms to the early Toarcian (Jurassic) oceanic anoxic event: environmental  
40  
41 1066 change and differential subsidence. *Sedimentology* **55**, 1011–1028.  
42  
43 1067 VELIĆ I., 2007, Stratigraphy and Palaeobiogeography of Mesozoic benthic foraminifera of the Karst  
44  
45 1068 Dinarides (SE Europe). *Geologia Croatica* **60**, 1–113.  
46  
47 1069 ZANFERRARI, A., MASETTI, D., MONEGATO, G. & POLI, M. E., 2013. Geological map and explanatory  
48  
49 1070 notes of the Italian Geological Map at the scale 1:50.000: Sheet 049 “Gemona del Friuli”. ISPRA -  
50  
51 1071 *Servizio Geologico d'Italia-Regione Autonoma Friuli Venezia Giulia*, 262  
52  
53 1072 pp.<http://www.isprambiente.gov.it/Med>.  
54  
55  
56  
57  
58  
59  
60

1  
2  
3 1073 ZHURAVLEV, A. Y. & WOOD, R.A., 2009. Controls on carbonate mineralogy: Global CO<sub>2</sub> evolution and  
4  
5 1074 mass extinctions. *Geology* **37**, 1123–1126.  
6  
7

8 1075  
9

10 1076  
11

12 1077  
13

14  
15 1078 FIGURE CAPTIONS  
16

17 1079 Fig. 1: A: Mesozoic structural domain of the Southern Alps. The dotted line indicates the section in Fig.

18  
19 1080 1B. B: Section across the Southern Alps showing the extensional Mesozoic architecture of the  
20

21 1081 Southern Alps at the end of Early Cretaceous time. After Masetti *et al.* (2012).  
22

23 1082 Fig. 2: The chemostratigraphic transect across different types of Jurassic successions inside the main  
24

25 1083 palaeogeographic units of the eastern Southern Alps and location of the sections presented here. In  
26

27 1084 the map, 1 and 2 represent, respectively, the areal distribution of central-western and the north-eastern  
28

29 1085 areas of the Trento Platform; 3 represents the Belluno Basin; 4 and 5 represent, respectively, the  
30

31 1086 northern and southern areas of the Friuli Platform. ZG = Monte Zugna Formation; OL = Loppio Oolitic  
32

33 1087 Limestone; RZ = Rotzo Formation; CG = Undifferentiated Calcari Grigi; OM = Massone Oolite; ENF =  
34

35 1088 Fanes Piccola Encrinite; OSV = San Vigilio Oolite + Tenno Formation; SOV = Soverzene Formation;  
36

37 1089 IGNE = Igne Formation; ARV = Rosso Ammonitico Veronese ; VJ = Vajont Limestone; CEL = Cellina  
38

39 1090 Limestone. Modified from Masetti *et al.* 2012.  
40

41 1091 Fig. 3: Lithostratigraphic relationships of the Jurassic units across the entire Trento Platform–Plateau  
42

43 1092 from the Lombardian Basin in the west, to the Belluno Basin in the east. Red spots highlight the location  
44

45 1093 of the negative CIE described in the text. Modified from Masetti *et al.* (2012).  
46

47 1094 Fig. 4: Monte Verzegnis and Monte Cumieli sections. In the upper part of the deep-water Monte  
48

49 1095 Verzegnis section there is an abrupt positive carbon-isotope excursion followed by a broad negative  
50

51 1096 excursion over the likely stratigraphical range of *Arnioceras*. In the shallow-water Monte Cumieli  
52

53 1097 section, the same two negative excursions are tentatively recognizable, the first just above the top of  
54

55  
56  
57  
58  
59  
60

1  
2  
3 1098 the peritidal unit of the Monte Zugna Formation and the second in the calcarenitic unit of the same  
4  
5 1099 formation, separated by a thin micritic intercalation corresponding to a positive CIE. LO *Paleomayncina*  
6  
7 1100 *termieri* indicates its lowest occurrence identified in the section.

9  
10 1101 Fig. 5: Ammonite stratigraphy of the Sinemurian Stage. Modified from Dommergues *et al.*, 1994.

11 1102 Fig. 6: Microfacies from Foza and Cumieli sections. a) micritic ooids showing thinly laminated outer  
12  
13 1103 tangential cortices, associated with *Palaeodasycladus mediterraneus*, visible in a transversal section in  
14  
15 1104 the lower part of the thin-section. Lower part of the calcarenitic unit of the Monte Zugna Fm., Foza  
16  
17 1105 section, scale bar = 1 mm; b) radial-fibrous ooids in which crystalline cortices are penetrated by dark  
18  
19 1106 microborings. *Everticyclammina praevirguliana* at the nucleus of the largest ooid. Upper part of the  
20  
21 1107 calcarenitic unit of the Monte Zugna Fm., Cumieli section, scale bar = 1 mm.

22  
23 1108 Fig. 7: Foza and Chizzola sections. In the Foza section the same two negative excursions described in  
24  
25 1109 the Mount Verzegnis section are readily discernible. The stratigraphically lowest negative excursion is  
26  
27 1110 present just above the base of the calcarenitic unit of the Monte Zugna Formation where the *Gervillia*  
28  
29 1111 bed crops out, and the stratigraphically higher negative excursion in the calcarenitic unit of the same  
30  
31 1112 formation. In the Chizzola section, the same isotopic pattern is repeated with the positive excursion  
32  
33 1113 coincident with the *Gervillia* bed, but outcrop failure does not allow generation of data from  
34  
35 1114 stratigraphically lower strata.

36  
37 1115 Fig. 8: Chemostratigraphic transect through the Eastern Southern Alps with pertinent biostratigraphic  
38  
39 1116 data. The figure illustrates the correlation of the above-described anomalies of the  $\delta^{13}\text{C}$  curves across  
40  
41 1117 the entire Eastern Southern Alps, from the Garda Lake to the eastern Italian border. The excellent  
42  
43 1118 matching between the single curves allows recognition, both in the shallow- and deep-water units, of  
44  
45 1119 the abrupt positive followed by broader negative carbon-isotope excursion described in the text. The  
46  
47 1120 correlation belt, coloured grey in the figure, defines the major negative excursion and its lower  
48  
49 1121 boundary (abrupt positive excursion) can be correlated with the peak of the excursion to heavier values  
50  
51 1122 in the *turneri* Zone: this level records the first appearance of the foraminifera *Paleomayncina termieri*.  
52  
53 1123 Recognition and proposed zonal attribution of key carbon-isotope excursions in Monte Verzegnis  
54  
55  
56  
57  
58  
59  
60

1  
2  
3 1124 derives from data from well-dated Sinemurian mudstones and shales from the UK (Fig. 8).  
4  
5 1125 Fig. 9: Left-hand diagram illustrates the Copper Hill Borehole (Eastern England) studied by Riding *et al.*  
6  
7 1126 (2012) and illustrating an increase of the dinoflagellate cyst *Liasidium variabile* and the thermophilic  
8  
9 1127 pollen grain *Classopollis classoides* in ammonite-bearing mudstones, suggesting the occurrence of a  
10  
11 1128 warming event coincident with a negative carbon-isotope excursion in marine and terrestrial organic  
12  
13 1129 matter largely corresponding to the *obtusum* and *oxynotum* Zones of the Sinemurian Stage. The  
14  
15 1130 presence of the negative excursion in terrestrial pollen indicates that the atmosphere as well as the  
16  
17 1131 ocean was affected by the disturbance in the carbon cycle. Scale in metres is depth below surface.  
18  
19 1132 *semicost.* = *semicostatum* Zone; *ob.* = *obtusum* Zone; *oxynot* = *oxynotum* Zone. Right-hand diagram  
20  
21 1133 illustrates high-resolution organic carbon-isotope stratigraphy of Sinemurian ammonite-bearing black  
22  
23 1134 shales from Dorset, Southern England (Weedon and Jenkyns, 2013). A positive excursion is  
24  
25 1135 characteristic of the *turneri* Zone followed by a negative excursion in the lower part of the *obtusum*  
26  
27 1136 Zone; the upper part of the *obtusum* Zone and the whole of the *oxynotum* Zone are lost to a hiatus.  
28  
29 1137 Grey band illustrates the position of the principal negative carbon-isotope excursion, only partly  
30  
31 1138 developed in Dorset. Depth is given in metres below the top of the Black Ven Marls. *semi.* =  
32  
33 1139 *semicostatum* Zone; *res.* = *resupinatum* Subzone; *obtu.* = *obtusum* Subzone; *rari.* = *raricostatoides*  
34  
35 1140 Subzone.  
36  
37  
38  
39  
40  
41 1141  
42  
43  
44  
45  
46  
47  
48  
49  
50  
51  
52  
53  
54  
55  
56  
57  
58  
59  
60

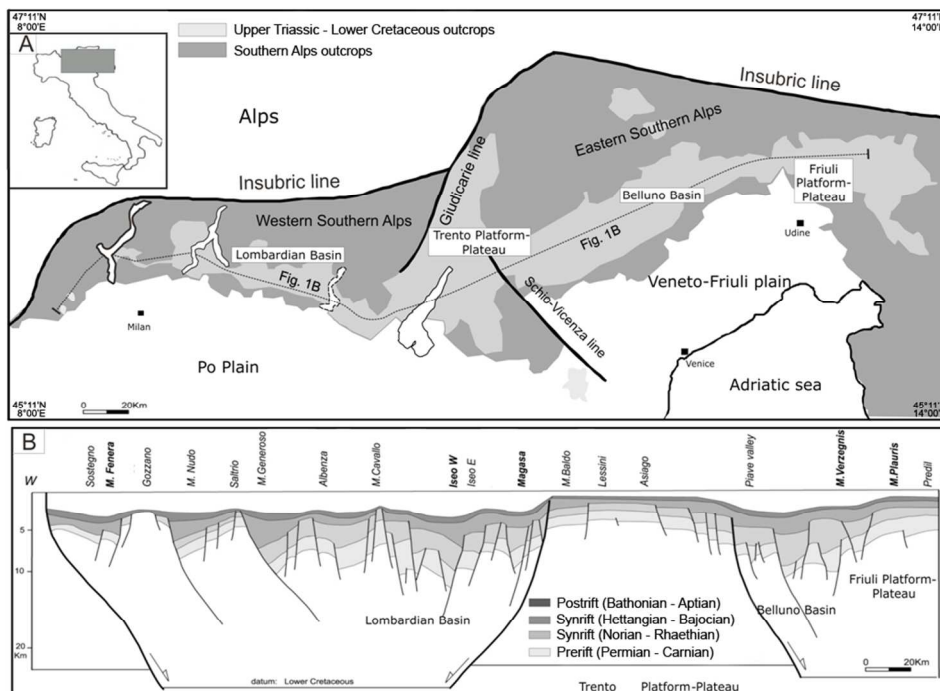


Fig. 1: A: Mesozoic structural domain of the Southern Alps. The dotted line indicates the section in Fig. 1B. B: Section across the Southern Alps showing the extensional Mesozoic architecture of the Southern Alps at the end of Early Cretaceous time. After Masetti et al. (2012). 184x137mm (150 x 150 DPI)

1  
2  
3  
4  
5  
6  
7  
8  
9  
10  
11  
12  
13  
14  
15  
16  
17  
18  
19  
20  
21  
22  
23  
24  
25  
26  
27  
28  
29  
30  
31  
32  
33  
34  
35  
36  
37  
38  
39  
40  
41  
42  
43  
44  
45  
46  
47  
48  
49  
50  
51  
52  
53  
54  
55  
56  
57  
58  
59  
60

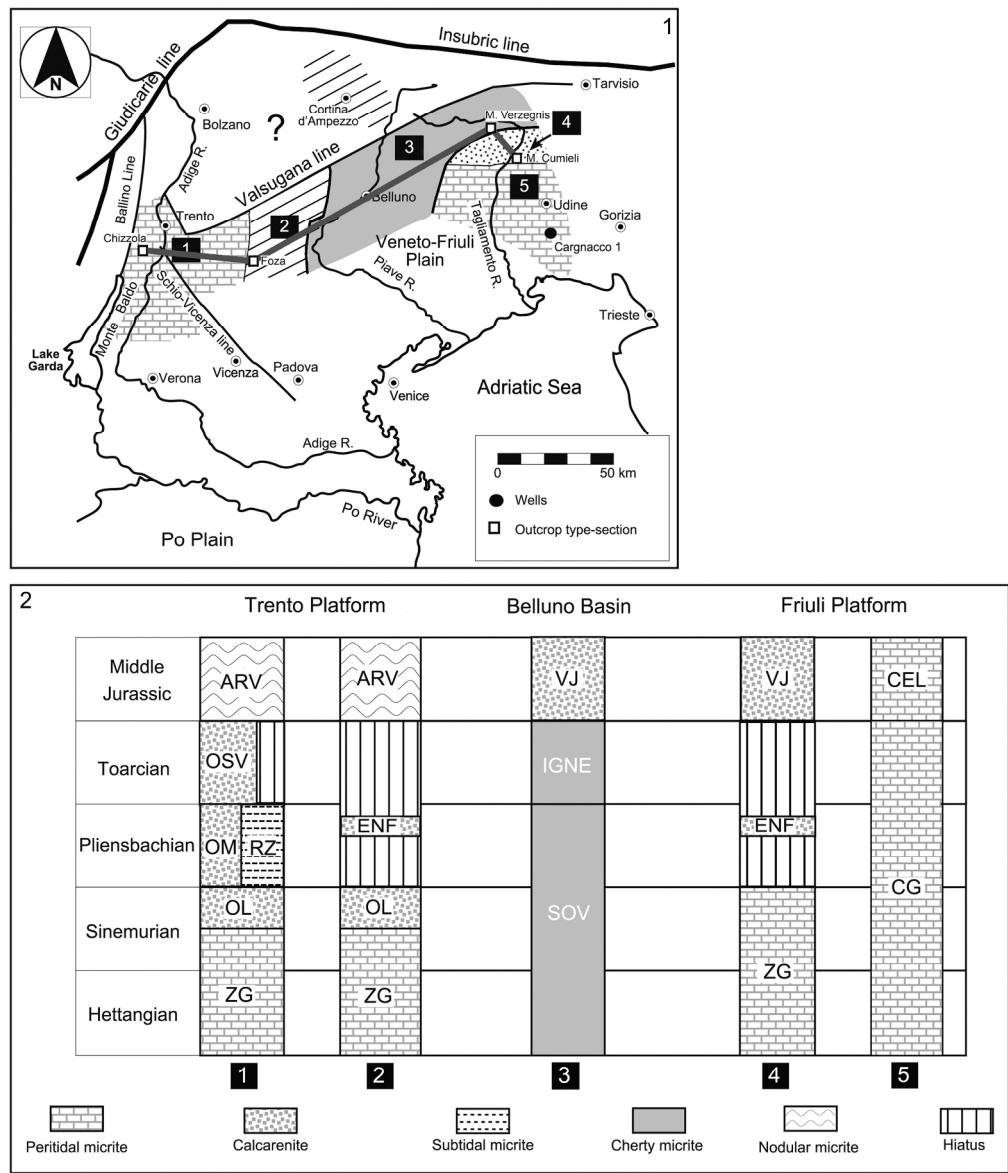


Fig. 2: The chemostratigraphic transect across different types of Jurassic successions inside the main palaeogeographic units of the eastern Southern Alps and location of the sections presented here. In the map, 1 and 2 represent, respectively, the areal distribution of central-western and the north-eastern areas of the Trento Platform; 3 represents the Belluno Basin; 4 and 5 represent, respectively, the northern and southern areas of the Friuli Platform-. ZG = Monte Zugna Formation; OL = Loppio Oolitic Limestone; RZ = Rotzo Formation; CG = Undifferentiated Calcarei Grigi; OM = Massone Oolite; ENF = Fanes Piccola Encrinite; OSV = San Vigilio Oolite + Tenno Formation; SOV = Soverzene Formation; IGNE = Igne Formation; ARV = Rosso Ammonitico Veronese ; VJ = Vajont Limestone; CEL = Cellina Limestone. Modified from Masetti et al. 2012.

220x257mm (300 x 300 DPI)

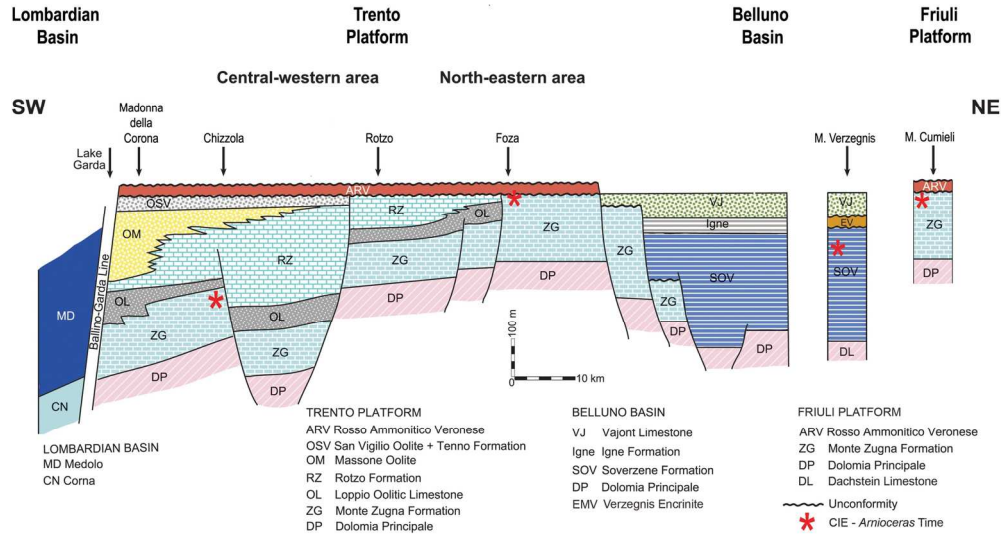


Fig. 3: Lithostratigraphic relationships of the Jurassic units across the entire Trento Platform–Plateau from the Lombardian Basin in the west, to the Belluno Basin in the east. Red spots highlight the location of the negative CIE described in the text. Modified from Masetti et al. (2012).

161x86mm (300 x 300 DPI)

or Review

1  
2  
3  
4  
5  
6  
7  
8  
9  
10  
11  
12  
13  
14  
15  
16  
17  
18  
19  
20  
21  
22  
23  
24  
25  
26  
27  
28  
29  
30  
31  
32  
33  
34  
35  
36  
37  
38  
39  
40  
41  
42  
43  
44  
45  
46  
47  
48  
49  
50  
51  
52  
53  
54  
55  
56  
57  
58  
59  
60



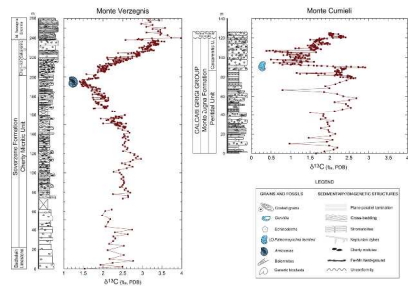


Fig. 4: Monte Verzegnis and Monte Cumieli sections. In the upper part of the deep-water Monte Verzegnis section there is an abrupt positive carbon-isotope excursion followed by a broad negative excursion over the likely stratigraphical range of *Arnioceras*. In the shallow-water Monte Cumieli section, the same two negative excursions are tentatively recognizable, the first just above the top of the peritidal unit of the Monte Zugna Formation and the second in the calcarenitic unit of the same formation, separated by a thin micritic intercalation corresponding to a positive CIE. LO *Paleomayncina termieri* indicates its lowest occurrence identified in the section.

296x124mm (300 x 300 DPI)

Or Review

1  
2  
3  
4  
5  
6  
7  
8  
9  
10  
11  
12  
13  
14  
15  
16  
17  
18  
19  
20  
21  
22  
23  
24  
25  
26  
27  
28  
29  
30  
31  
32  
33  
34  
35  
36  
37  
38  
39  
40  
41  
42  
43  
44  
45  
46  
47  
48  
49  
50  
51  
52  
53  
54  
55  
56  
57  
58  
59  
60

STAGE	Ammonite Zone	Ammonite Subzone
UPPER SINEMURIAN	<i>raricostatum</i>	<i>aplanatum</i>
		<i>macdonnelli</i>
		<i>raricostatum</i>
		<i>densinodulum</i>
	<i>oxynotum</i>	<i>oxynotum</i>
		<i>simpsoni</i>
	<i>obtusum</i>	<i>denotatus</i>
		<i>stellare</i>
		<i>obtusum</i>
LOWER SINEMURIAN	<i>turneri</i>	<i>birchi</i>
		<i>brooki</i>
	<i>semicostatum</i>	<i>sauzeanum</i>
		<i>scipionianum</i>
		<i>lyra</i>
	<i>bucklandi</i>	<i>bucklandi</i>
		<i>rotiforme</i>
		<i>conybeari</i>

Amioceras Time

Fig. 5: Ammonite stratigraphy of the Sinemurian Stage. Modified from Dommergues et al., 1994.  
242x466mm (300 x 300 DPI)

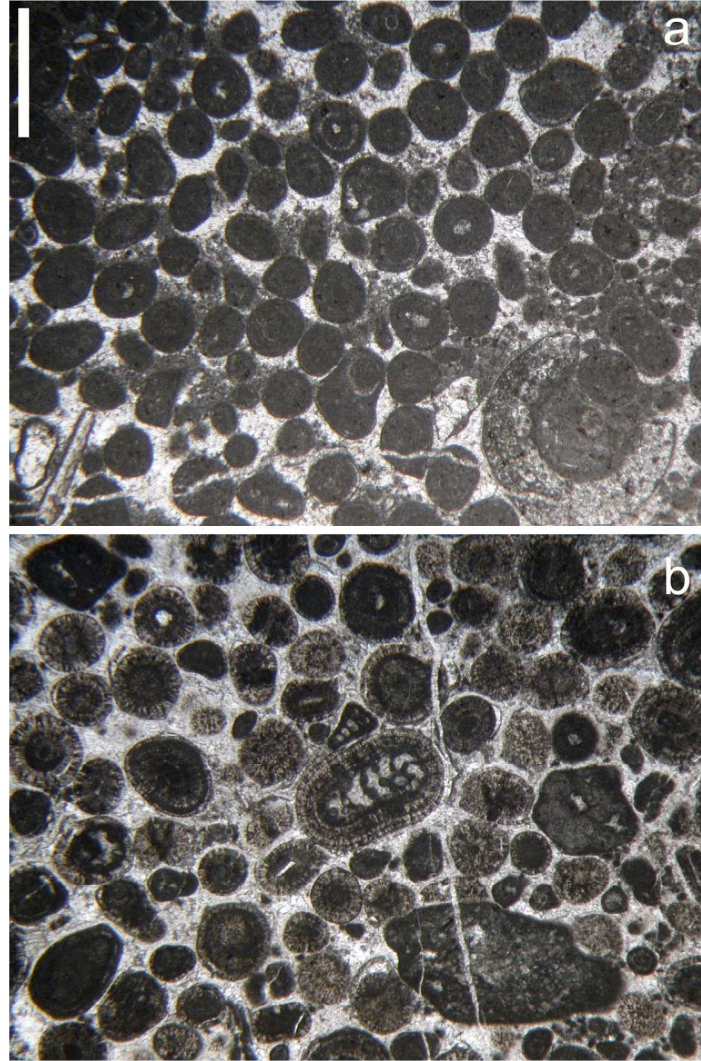


Fig. 6: Microfacies from Foza and Cumieli sections. a) micritic ooids showing thinly laminated outer tangential cortices, associated with *Palaeodasycladus mediterraneus*, visible in a transversal section in the lower part of the thin-section. Lower part of the calcarenitic unit of the Monte Zugna Fm., Foza section, scale bar = 1 mm; b) radial-fibrous ooids in which crystalline cortices are penetrated by dark microborings. *Everticyclammina praevirguliana* at the nucleus of the largest ooid. Upper part of the calcarenitic unit of the Monte Zugna Fm., Cumieli section, scale bar = 1mm.  
297x419mm (300 x 300 DPI)

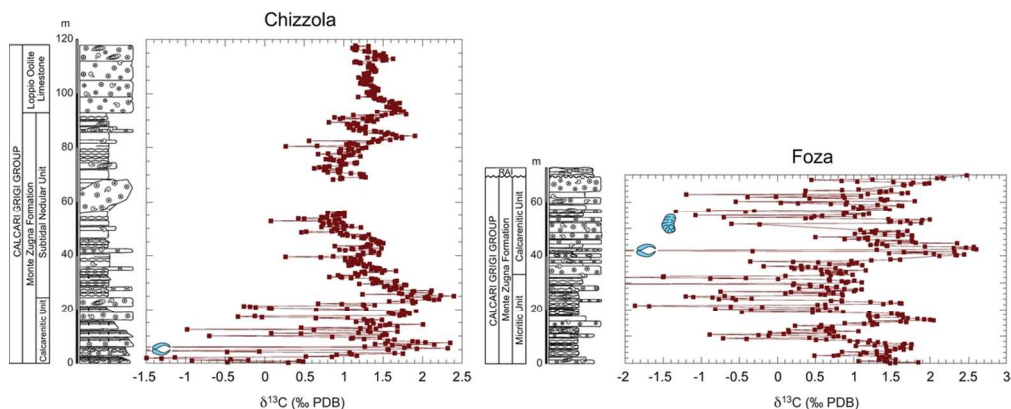


Fig. 7: Foza and Chizzola sections. In the Foza section the same two negative excursions described in the Mount Verzegnis section are readily discernible. The stratigraphically lowest negative excursion is present just above the base of the calcarenitic unit of the Monte Zugna Formation where the Gervillia bed crops out, and the stratigraphically higher negative excursion in the calcarenitic unit of the same formation. In the Chizzola section, the same isotopic pattern is repeated with the positive excursion coincident with the Gervillia bed, but outcrop failure does not allow generation of data from stratigraphically lower strata.

105x42mm (300 x 300 DPI)

For Review

1  
2  
3  
4  
5  
6  
7  
8  
9  
10  
11  
12  
13  
14  
15  
16  
17  
18  
19  
20  
21  
22  
23  
24  
25  
26  
27  
28  
29  
30  
31  
32  
33  
34  
35  
36  
37  
38  
39  
40  
41  
42  
43  
44  
45  
46  
47  
48  
49  
50  
51  
52  
53  
54  
55  
56  
57  
58  
59  
60

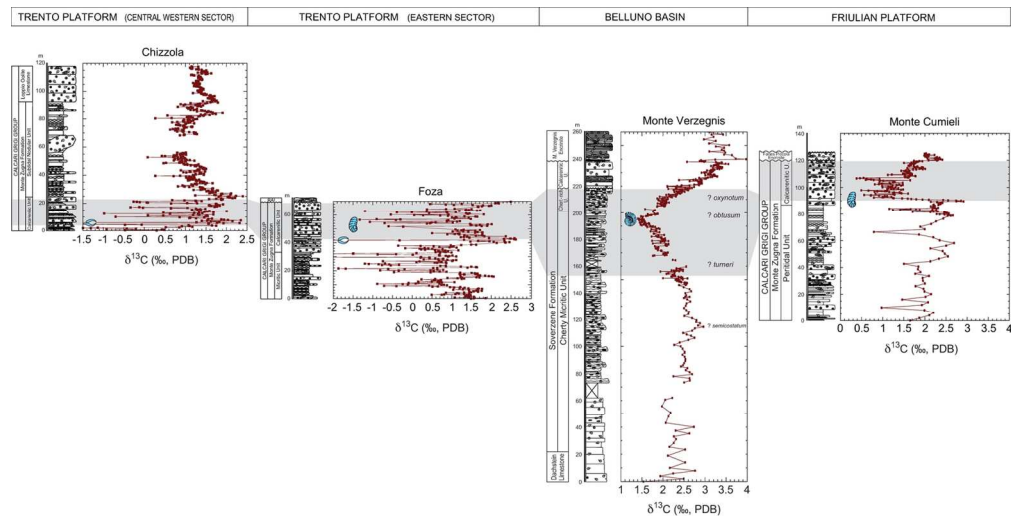


Fig. 8: Chemostratigraphic transect through the Eastern Southern Alps with pertinent biostratigraphic data. The figure illustrates the correlation of the above-described anomalies of the  $\delta^{13}\text{C}$  curves across the entire Eastern Southern Alps, from the Garda Lake to the eastern Italian border. The excellent matching between the single curves allows recognition, both in the shallow- and deep-water units, of the abrupt positive followed by broader negative carbon-isotope excursion described in the text. The correlation belt, coloured grey in the figure, defines the major negative excursion and its lower boundary (abrupt positive excursion) can be correlated with the peak of the excursion to heavier values in the *turneri* Zone: this level records the first appearance of the foraminifera *Paleomayncina termieri*. Recognition and proposed zonal attribution of key carbon-isotope excursions in Monte Verzegnis derives from data from well-dated Sinemurian mudstones and shales from the UK (Fig. 8).  
142x72mm (300 x 300 DPI)

Review

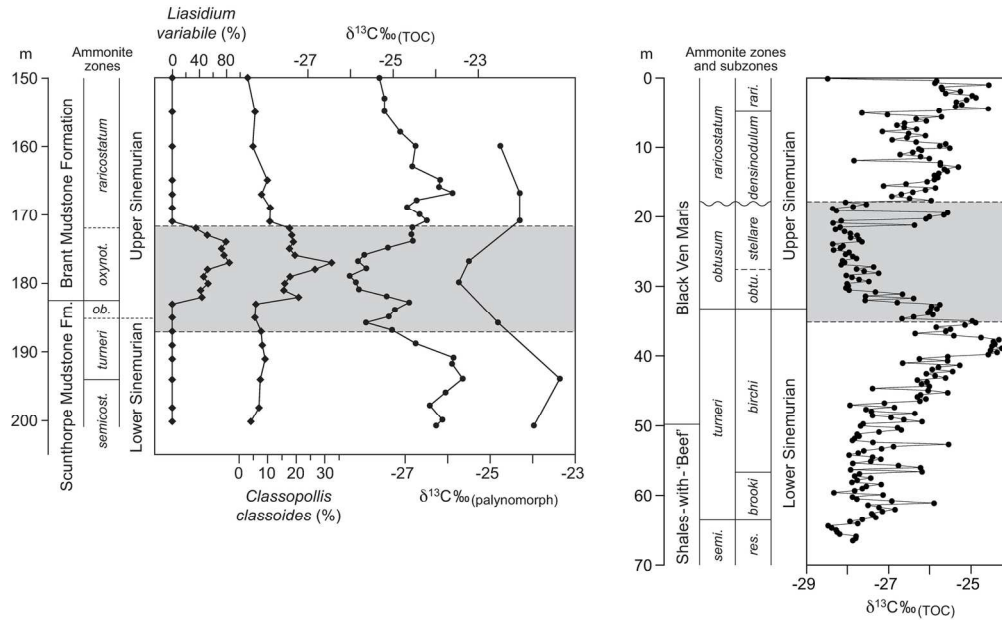


Fig. 9: Left-hand diagram illustrates the Copper Hill Borehole (Eastern England) studied by Riding et al. (2012) and illustrating an increase of the dinoflagellate cyst *Liasidium variabile* and the thermophilic pollen grain *Classopollis classoides* in ammonite-bearing mudstones, suggesting the occurrence of a warming event coincident with a negative carbon-isotope excursion in marine and terrestrial organic matter largely corresponding to the obtusum and oxynotum Zones of the Sinemurian Stage. The presence of the negative excursion in terrestrial pollen indicates that the atmosphere as well as the ocean was affected by the disturbance in the carbon cycle. Scale in metres is depth below surface. semicost. = semicostatium Zone; ob. = obtusum Zone; oxynot = oxynotum Zone. Right-hand diagram illustrates high-resolution organic carbon-isotope stratigraphy of Sinemurian ammonite-bearing black shales from Dorset, Southern England (Weedon and Jenkyns, 2013). A positive excursion is characteristic of the turneri Zone followed by a negative excursion in the lower part of the obtusum Zone; the upper part of the obtusum Zone and the whole of the oxynotum Zone are lost to a hiatus. Grey band illustrates the position of the principal negative carbon-isotope excursion, only partly developed in Dorset. Depth is given in metres below the top of the Black Ven Marls. semi. = semicostatium Zone; res. = resupinatum Subzone; obtu. = obtusum Subzone; rari. = raricostatoides Subzone.

161x99mm (300 x 300 DPI)



1  
2  
3  
4  
5  
6  
7  
8  
9  
10  
11  
12  
13  
14  
15  
16  
17  
18  
19  
20  
21  
22  
23  
24  
25  
26  
27  
28  
29  
30  
31  
32  
33  
34  
35  
36  
37  
38  
39  
40  
41  
42  
43  
44  
45  
46  
47  
48  
49  
50  
51  
52  
53  
54  
55  
56  
57  
58  
59  
60